THRUST CONTROL DESIGN FOR UNMANNED MARINE VEHICLES

A Thesis Submitted to
the Graduate School of Engineering and Sciences of
İzmir Institute of Technology
in Partial Fulfillment of the Requirements for the Degree of

MASTER OF SCIENCE

in Mechanical Engineering

by
Buğra ALKAN

April 2012
İZMİR

We approve the thesis of **Buğra ALKAN**

Assist. Prof. Dr. Mehmet İsmet Can DEDE
Supervisor

Assist. Prof. Dr. Ünver ÖZKOL
Co-Supervisor

Assoc. Prof. Dr. Serhan ÖZDEMİR
Committee Member

Prof. Dr. Nuri Süha BAYINDIR
Committee Member

Assist. Prof. Dr. Şevket GÜMÜŞTEKİN
Committee Member

09 April 2012

Prof. Dr. Metin TANOĞLU
Head of the Department of
Mechanical Engineering

Prof. Dr. R. Tuğrul SENGER
Dean of the Graduate School of
Engineering and Sciences

ACKNOWLEDGMENTS

I would like to express my gratitude to my advisor Asst. Prof. Dr. Mehmet İsmet Can Dede and my co-advisor Asst. Prof. Dr. Ünver Özkol for their invaluable advice, guidance, and encouragement.

I would like to thank the both İYTE Robotics and Fluid Mechanics laboratory staff for their help during my study.

I am also grateful to my parents for their endless support during my thesis and all of my life.

ABSTRACT

THRUST CONTROL DESIGN FOR UNMANNED MARINE VEHICLES

In conventional electrically driven propulsion systems with fixed pitch propellers, thruster controllers are usually aimed at controlling propeller shaft speed only. Especially in unmanned marine vehicles which operate in dynamic flow conditions, these type thruster controllers provide unsatisfactory thrust responses. The reason for this is that the thrust force is simultaneously affected by dynamic effects like, variable ambient flow velocity and angle, thruster-thruster interaction and ventilation. It is aimed to achieve acceptable thrust tracking accuracy in all kind of dynamic flow conditions in this thesis work. A novel feed-back based thruster controller which includes the effect of incoming axial flow velocity, is designed for this purpose. In controller design, first, thruster propeller's open water characteristics in four-quadrant flow states are measured. Data collected from open water tests are then non-dimensionalized and embedded in the controller's thrust model code. Relation between ideal shaft speed and desired thrust is derived by using the four-quadrant propeller model. The proposed method is evaluated in the experimental test-setup designed for this study to simulate open water conditions. Results indicate that thrust tracking performance of novel controller is acceptable in all four-quadrant flow tests.

ÖZET

İNSANSIZ DENİZ ARAÇLARI İÇİN İTİŞ DENETLEYİCİSİ TASARIMI

Elektrik tahrikli itiş sistemlerinin denetleyicileri, genelde yalnızca pervane şaft hızını denetlemeyi amaçlamaktadırlar. Değişken çevresel akış hızı ve açısı, iticiler arası etkileşim, ventilasyon gibi dinamik effektler, itme kuvvetini etkilemektedirler. Bununla beraber özellikle bu gibi dinamik akış koşullarında çalışan insansız deniz araçlarında, bu tür denetleyicilerin kullanılması verimsiz sonuçlar vermektedir. Bu tez çalışmasında, her tür dinamik akış koşulunda, sistemin itme kuvveti isteğinin kabul edilebilir bir ölçüde gerçeklemmesi amaçlanmaktadır. Bu amaçla eksenel su hızını değerlendirebilen yeni bir geri beslemeli itici denetleyicisi tasarlanmıştır. Çalışma sırasında, önce pervanenin dört çeyreklik akış koşullarında verdiği açık su karakteristikleri hesaplanmıştır. Açık su testlerinde elde edilen veriler boyutsuzlaştırılarak denetleyicinin itme kuvveti modeline eklenmiştir. Dört çeyrekli pervane modeli kullanılarak istenilen itme kuvveti ve ideal pervane şaft hızı arasında bir bağıntı türetilmiştir. Bir deney düzeneği açık su koşullarını gerçekleyebilmek için tasarlanmıştır. Sonuçlar, önerilen itiş sistemi denetleycisinin tüm dört çeyrek akış koşulunda kabul edilebilir sonuçlar verdiğini ortaya koymuştur.

TABLE OF CONTENTS

LIST OF FIGURES

Figure **Page**

LIST OF TABLES

Table **Page**

LIST OF SYMBOLS

Abbreviations

AUV	Autonomous Underwater Vehicle
CPP	Controllable Pitch Propeller
CRP	Contra-Rotating Propeller
FPP	Fixed Pitch Propeller
GNC	Guidance, Navigation and Control
GPS	Global Positioning System
P	Power (Control)
PID	Proportional-Integral-Derivative
PMS	Power Management System
Q	Torque (Control)
ROV	Remotely Operated Vehicle
S	Speed (Control)
UMV	Unmanned Marine Vehicle
USV	Unmanned Surface Vehicle

Lowercase

e_v	Shaft Speed Error	rps
f_Q	Propeller Torque Model	-
f_T	Propeller Thrust Model	-
h	Propeller Shaft Submergence	m
i_m	Motor current	A
i_f	Feed-forward Motor current	A
i_o	Open Loop Motor current	A
k_f	Motor Friction Coefficient	Nm.s/rps
k_m	Motor Torque Constant	Nm/A
n	Propeller Shaft Speed	rps

n_a	Actual Propeller Shaft Speed	rps
n_i	Ideal Propeller Shaft Speed	rps
t	Time	s
t_d	Differential Time	s
u	Vehicle Surge Speed	m/s
w	Wake Fraction Coefficient	-

Uppercase

A_P	Propeller Disc Area	m^2
D	Propeller Diameter	m
J	Advance Number	-
K_P	PD Controller Proportional Gain	-
K_Q	Torque Coefficient	-
K_{Q0}	Nominal Torque Coefficient	-
K_T	Thrust Coefficient	-
K_{T0}	Nominal Thrust Coefficient	-
P	Propeller Power	W
P_n	Nominal Propeller Power	W
Q	Propeller Torque	Nm
T	Thrust	N
T_a	Actual Thrust	N
T_d	Desired Thrust	N
T_n	Nominal Propeller Thrust	N
V_a	Propeller Advance (Inflow) Velocity	m/s
V_p	Flow Velocity Through the Propeller Disc	m/s

Greek

α	Propeller Feed-forward Control Constant	Nm/N
η	Propeller Efficiency	-

η_0	Nominal Propeller Efficiency	-
ρ	Density of Water	Kg/m^3

CHAPTER 1

INTRODUCTION

Recent advances in communication, artificial intelligence, energy and propulsion systems are being applied to develop technologies that will lead far more efficient ways of intervention, surveillance and investigation in oceans. There is an increasing interest in the design and development of Unmanned Underwater Vehicles (UMVs) as a part of these advances in ocean technologies. UMVs are used in a wide range of applications in oceans and some of these applications require precise vehicle control especially in critical tasks. Thruster control, which is the lowest layer of the control loop of the system (Kim et al. 2005) gained more attention in scientific world to develop vehicles with acceptable operation performances. A variety of control methods are proposed by researchers in order to obtain satisfactory performances from vehicles' thrusters.

This thesis focuses on the control of a screw-type propeller-driven electrical thruster through velocity feedback for UMVs. The aim in the propulsion control is to achieve high thrust production accuracy. UMV types and applications, their propulsion methods and control structures are investigated to comprehend the fundamentals of subject and understanding of the propulsion problems.

1.1. Unmanned Marine Vehicles

UMVs are marine robots which are operated with minimum or without intervention of human operator. Vehicles range in size from man portable lightweight UMVs to large diameter vehicles of over 12 meter length especially in unmanned surface vehicles (USVs) (Roberts et al. 2006).

Primarily in oceanographic researches, UMVs carry sensors for many reasons such as navigation, guidance and data collection. Typical sensors include compasses, depth sensors, side scans and acoustic sensors, magnetometers, thermistors and conductivity probes (Blanke et al. 2000).

Most UMVs are powered by rechargeable batteries while some vehicles especially larger ones from remotely operated vehicles (ROVs) and autonomous

underwater vehicles (AUVs) are powered by aluminum-based semi-fuel cells. Diesel engines are generally selected as a main power choice for large USVs (Guibert et al. 2005).

For body construction, conventional ROVs are built with a large flotation pack on top of an aluminum chassis. Synthetic foam is generally used for the flotation. AUVs' body structure is generally torpedo shaped in order to decrease power consumption over long cruises since they have limited power storage. USVs structures are generally like high-speed off-shore boats and do not contain any limitation (Lindegaard et al. 2003).

In UMVs, thrusters commonly rely on lip-seals in order to protect motor internals from corrosion. Also ROVs' tethering cables run inside oil-filling tubing because of the same reason.

In many UMVs, cameras, a variety of sensors and manipulators can be integrated for intervention, surveillance and investigation tasks.

1.1.1. Types and Applications

UMV definition includes autonomous underwater vehicles (AUV), remotely operated vehicles (ROV), and unmanned surface vehicles (USV). The UMV types and their applications are briefly explained in the following subsection.

1.1.1.1. Autonomous Underwater Vehicles

AUVs are robots that travel underwater without requiring input from an operator. AUVs are used for a wide range of tasks with different roles and missions. Oil and gas industries commonly use AUVs to make detailed map of the seafloor before they build subsea infrastructures so pipelines and subsea completions can be installed in the most cost-effective manner with minimum disruption to environment (Akçakaya et al. 2009). On the other hand, AUVs are also used for different application areas such as military, science and hobby. A typical military mission for an AUV is to map an area to determine if there are enemy mines and manned submarines or to monitor protected area for unwanted objects (Hardy et al. 2008). For scientific purpose, the ability of deploying an AUV to missions over long distances without surface aid has major

advantages for science. Missions with AUVs are now carried out, seeking knowledge to improve one's understanding of global climatology, marine ecology and geology of ocean bed (Society of Underwater Technologies 2012). Also this type of vehicles can be used in seismic activity research, seabed geo-technics and ocean current analysis. In 2011, National Aeronautics Space Administration (NASA) launched a probe carrying a sophisticated cryobot and an AUV in order to seek life in Jupiter's moon Europa's icy oceans which is an excellent example of the importance of AUVs for science (Bortz 2010).

A torpedo shaped AUV which is used in under-ice missions to gather valuable data about climate changes on Earth is presented in Figure 1.1.

Figure 1. 1. Bluefin 21 Bp autonomous underwater vehicle
(Source: Indian Defense Review 2012)

1.1.1.2. Remotely Operated Vehicles

ROV is the common accepted name for tethered underwater robots in the offshore industry. Different from AUVs, ROVs are tele-operated robots, highly maneuverable and operated from a command center. They are linked to command center by a tether which is a group of cables that carry electrical power, video and data signals back and forth between the operator and vehicle. Most ROVs are equipped with at least a video camera and lights. Additional equipments are commonly added to the vehicle to expand its capabilities.

ROVs can be used in a wide range of complex missions similar to AUV applications. ROVs are primarily deployed for underwater salvage, inspections, installations and repair tasks and can also be used for naval, scientific and educational purposes such as; mine neutralization, marine ecology inspections, iceberg profiling, oceanographic sampling, and underwater photography (Petersen 2009). A picture which is taken from ROV exploration mission at Kawai Barat submarine volcano is presented in Figure 1.2.

Figure 1. 2. Science class ROV
(Source: National Oceanic and Atmospheric Administration 2012)

In addition to ordinary duties of these vehicles, ROVs may also be used in emergency situations where intervention tasks are required. On August, the 4th, 2005, in the Pacific sea, near Kamchatka, at depth of 200 meters, a Russian manned submarine Prizz Class AS-28 got stuck into the cables of underwater radar. One day later British ROV named Scorpio was there and able to cut the cables thus allowing the submarine to surface safely (Antonelli et al. 2006).

Another emergency scenario occurred during the Gulf of Mexico oil spill environmental crisis. On the 20th of April 2010, Deepwater Horizon offshore oil drilling rig operated by British Petroleum (BP) exploded and sank. Oil began leaking at a rate of 2.5 million gallon per day, resulting in a massive environmental degradation. Engineers sent two ROVs in order to investigate the area. In spite of their failure on closing the blowout preventer valves on the wellhead, these vehicles made important contributions to the conduct of the operation and succession of the mission (Monster and Critics

News 2012). A picture from Mexico Gulf oil spill ROV operation is presented in Figure 1.3.

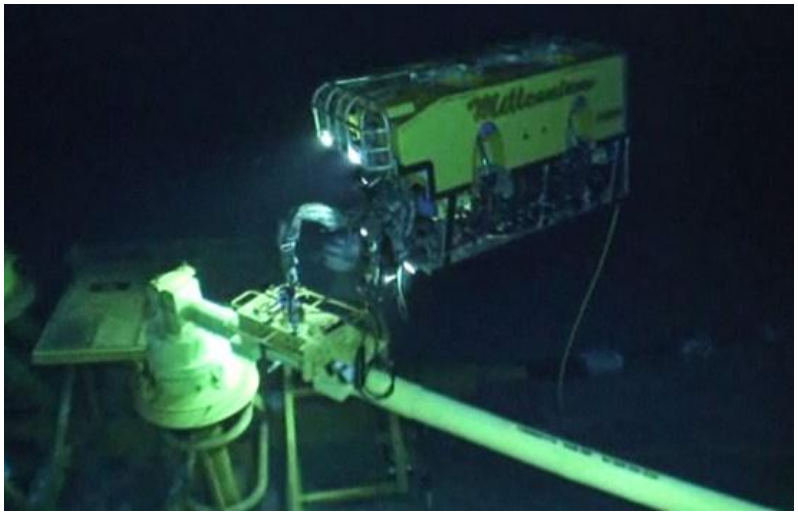

Figure 1. 3. Work class ROV
(Source: Monster and Critics News 2012)

1.1.1.3. Unmanned Surface Vehicles

Another type of UMV is USV which operates on the surface of the water without a crew and can be tele-operated or autonomously navigated. Common applications of USVs are port and infrastructure security, coastal patrolling, search and rescue operations and logistic purposes (Corfield 2002). An autonomously navigated USV from United States Navy is presented in Figure 1.4.

Figure 1. 4. A naval USV
(Source: Defense and Industry News 2012)

1.1.2. Vehicle Propulsion

UMV types and areas of application demand for precision in critical tasks that were mentioned in the previous section. The propulsion technology is one of the key elements in providing precise operation of these vehicles.

UMVs have propulsion units and rely on these to conduct stabilization, maneuvering, and movement.

In literature, UMV propulsion units are divided into three main categories which are propeller driven electrical thrusters, hydraulic pump jets and biomimetic propulsion mechanisms (Roberts et al. 2006).

1.1.2.1. Propeller-Driven Electrical Thrusters

Propeller-driven type of propulsion systems are the most common ones among the UMVs. Motor, seals, propellers and ducts constitute the main components of a typical electrical thruster. These components can be modified depending on the operation conditions of UMV. Generally, there are two main types of motor used in electrical thruster. Thruster design in both is similar; however one uses brushless DC motors and the other brushless AC motors. In both cases, brushless motors are used due to the fact that regular permanent magnet motors require the transfer of electricity from brushes to central coil and brushes wear out in time. A typical ducted electrical thruster from CMC Marine Company is presented in Figure 1.5.

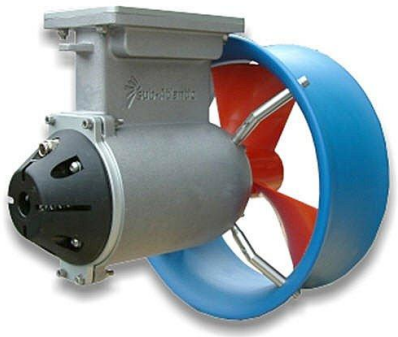

Figure 1. 5. Propeller based ducted electrical marine thruster
(Source: Powersys Company 2012)

Various types of propulsion units exist, as well as different types of propellers. The most common types of propellers are fixed pitch propellers (FPP), controllable pitch propellers (CPP) and contra-rotating propellers (CRP) (Smogeli 2006). The thrust produced by FPP and CRP can only be controlled by propeller speed whereas in CPP thrust can be controlled by both propeller speed and blade angles (pitch). All propeller types can be ducted or open. On a ducted propeller, propeller is centered by a duct or nozzle which increases the efficiency of UMV on both low and high operation speeds.

1.1.2.2. Hydraulic Pump Jets

Hydraulic pump jets are marine propulsion systems that generate jet of water for propulsion. The mechanical arrangement includes a ducted propeller with nozzle or a centrifugal pump and a nozzle. This type of propulsion systems has some advantages over propeller-based ones for certain applications. In high speed and shallow draft operations, hydraulic pump jets are commonly selected as propulsion units, especially in USVs (King 1998).

1.1.2.3. Biomimetic Propulsion Mechanisms

Efficient usage of the energy stored to the batteries before the mission has a great importance in AUVs which are designed for long-term missions. Propulsion mechanisms inspired by sea-creatures and birds provide a solution for the energy efficiency problem. Energy efficiency of biomimetic mechanisms are generally rated better compared to pump jets or propeller type thrusters (Cohen 2006).

There are several types and shapes of biomimetic propulsion mechanisms such as fin-like, wing-like or webbed feet-like. Fin-like mechanisms or in other words biomimetic fin actuators are usually used in AUVs for their energy efficiency, but they cannot produce high thrust as pump jets or propeller type thrust. Passive flexible fin actuator schematics are illustrated in Figure 1.6.

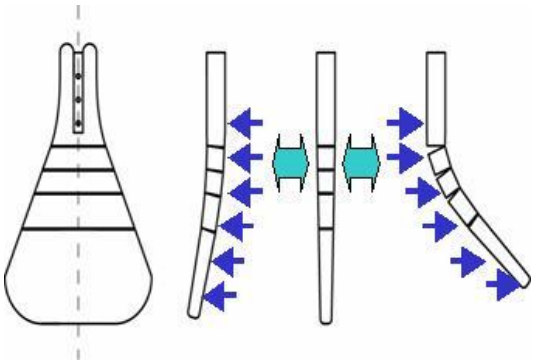

Figure 1. 6. Biomimetic fin actuators
(Source: Osaka University 2012)

1.1.3. Vehicle Control Structure

The control structure of a UMV is crucial for reliability in completing a mission. In literature, the real-time control structure of a UMV's guidance, navigation and control system, is divided into three layers (Smogeli 2006):

- The guidance and navigation layer (Local set point and routes)
- The high-level plant control layer (Power management and thrust allocation)
- The low-level thruster control layer (Propulsion control)

The guidance and navigation layer include sensors and vehicle observers. This layer may have functions like low speed tracking, set point chasing and route planning (Smogeli 2006).

The high-level controller that receives commands from a joystick (ROV) or an autonomous path planner (AUV) computes the forces and moments that in all directions that can be achieved by vehicle needed to counteract environmental loads in order to track the desired route. The thrust allocation system calculates thrust set points for each propulsion unit according to given optimization criterion (Smogeli 2008). On the other hand power management systems minimize the consumption of power, which is especially critical in AUVs.

The low-level thrust controllers control the thrusters according to thrust set points which are provided by from thrust allocation systems (Kim et al. 2005).

1.2. Problem Statement

The stated problems in this section are on the low-level thrust controllers. Measurement of the actual propeller thrust is generally not available or expensive due to requirement of force transducers on the vehicle. The mapping from desired thrust to actual thrust without any feedback is not reliable because of the thrust force, which is produced by vehicle's thrusters, is simultaneously affected by motor and shaft model, propeller characteristics, vehicle's motions and speed, ocean currents etc. (Ruth 2002). Therefore, if the low-level control has unacceptable performance, the stability, maneuverability and positioning will be affected (Ruth 2002).

Thrusters work in a wide range of operating conditions. The thrust demand in UMVs, will increase or decrease with the severity of the environmental conditions but in most cases thruster controllers are designed for operation in flat surface conditions. The controllers are generally in open-loop structure not dealing with dynamic effects that cause fluctuations in the thrust force. Large thrust losses may occur in harsher conditions if the effects of these conditions are not accounted for.

The main problem statement is formulated as follows:
"Given a desired thrust and an unknown flow scenario and operation depth, how can the propeller be controlled in order to:

- Achieve good trust tracking accuracy,
- Maintain acceptable high and low speed maneuverability,
- Avoid unnecessary power consumptions,
- And at the same time have reliable performance?

1.3. Objectives of Thesis

Consistent with the problem statement, the aim of this thesis is to design a thrust control system for a propeller-based electrical thruster that provides acceptable trust tracking accuracy in both calm and extreme UMV operation conditions. Controller of the thruster will deal with ambient flow that simulates a UMV navigating in open water conditions. The navigation direction will vary while the thrust direction magnitude changes to evaluate the controller for all possible conditions. An experimental test set-

up is to developed to conduct the experiments in laboratory setting within the aim of thesis. Overall, the control system for the thruster is to be developed that provide acceptable results for all navigation conditions created in the test set-up.

1.4. Organization of Thesis

Modeling and control of a propeller-based electrical driven marine propeller are investigated in this thesis work. Chapter 2 provides a review of the literature on thrust control algorithms and tests. In this chapter, common thrust controller algorithms are described and related studies based on four-quadrant model-based control algorithm are examined. Chapter 3 introduces the methodologies that are used on open water performance and thrust control tests. In this chapter, experimental test-setup, flow monitoring and shaft speed measurement methods are presented. Also results from open-water characteristics of a model scale propeller are examined. Chapter 4 gives information about the proposed thrust controller. In chapter 5, the thrust control tests are presented in both variable advance velocity and quasi-static conditions and the results are discussed. Finally, conclusions are given and future works are addressed in the last chapter.

CHAPTER 2

LITERATURE SURVEY

The controls of UMVs in different tasks present several challenges due to a number of factors. This is mainly caused by nonlinearity of vehicle dynamics. Many uncertainties result in inaccurate prediction, or calculation of hydrodynamic coefficients. Meanwhile additional disturbances from the environment increase the uncertainty level.

Various control techniques have been proposed for UMVs which are tested in both simulation and actual open water experiments since 1970 onward. Fuzzy control, reinforcement learning, model predictive, neural networks, hybrid, back stepping, adaptive, PID and LQG/LTR (Budiyono at al. 2009) controllers are the most common methods. Model-based control designs can be divided into three different approaches (Sugama et al. 2009).

- Model-based nonlinear control
- Model-based linear control
- Control without system model

Since there are lots of different approaches of propeller based thruster core low-level control, the literature survey is limited to model-based linear control. In this section advances in marine vehicle thruster control are reviewed in the section 2.1 followed by similar studies with respect to the studies conducted in this thesis are described in section 2.2.

2.1. State of the Art

Smogeli stated that “shaft speed control is achieved through conventional methods for electrically driven propellers and the origin of PID type controllers for propeller shaft speed control is uncertain, but they have probably been utilized for as long as conventional propellers have been used” (Smogeli 2006).

For unmanned underwater vehicles, both shaft speed control (Healey et al. 1993, Egeskov et al. 1995, Caccia et al. 2000, Sørensen et al. 2004, Roberts et al. 2004) and torque control (Yang et al. 1999, Antonelli et al. 2001, Whitcomb et al. 2004) have been used. According to Yoerger, "the predominating solution for underwater vehicles until 1990s was torque control" (Yoerger et al. 1991). He found that the thruster dynamics had a strong influence on the closed-loop underwater vehicle behaviors (Yoerger et al. 1991). Researchers proposed several low-level thrust controllers, all based on torque control of the thruster motor. The investigation on model-based thruster control for underwater vehicles was continued by Whitcomb and Yoerger's studies (Yoerger et al. 1999). They compared a torque controller with a high-gain proportional propeller shaft velocity controller with axial flow compensation. They concluded that "the torque controller was unacceptable for low thrust commands but with improved performance for higher thrust commands" (Yoerger et al. 1999). The high-gain shaft speed controller was shown to have poor performance, but gave good results with the addition of the axial flow compensation according to Yoerger's study (Yoerger et al. 1999). Continuing the concept of axial flow compensation, Fossen and Blanke (Blanke et al. 2000) proposed a nonlinear output feedback propeller shaft speed controller, with advance velocity estimator. The advance velocity estimator was designed based on the vehicle hydrodynamics and a model of the flow dynamics. According to Fossen and Blanke, "Results from this study were mainly applicable to an underwater vehicle with one propeller operating positive shaft rotation and vehicle speed condition" (Blanke et al. 2000). Tsukamoto et al. presented an experimental comparison study of five thruster control systems for underwater robots: on-line neural network control, off-line neural network control, fuzzy control, adaptive-learning control, and PID control (Tsukamoto et al. 1997). The controllers were based on direct control of the vehicle navigation direction using one thruster. Neural networks, fuzzy control, and adaptive-learning controls can also be found in the literature of UMV low-level thrust controller.

2.2. Experimental Thrust Control Studies

Experimental thrust control studies which include model-based thrust control algorithms with or without feedback gain are investigated in this section of chapter in order to highlight advantages and disadvantages of the available solution methods of

propulsion problem on UMVs. Section is divided into two groups as; experiments at zero and non-zero advance velocity.

2.2.1. Experiments at Zero Advance Velocity

Low-level thruster controllers must include dynamic flow models, due to vehicle's movement and ocean currents with different velocity and directions, which affect the speed of incoming flow through propeller disc. Produced thrust can increase or decrease even at the same propeller rotation speeds because of this reason (Kim et al. 2005). To design a controller that will deal with these dynamic flow effects, propeller reactions at zero incoming flow conditions must be examined.

Louis L. Whitecomb and Dana R. Yoerger's thruster low-level controllers based on linear flow models from Massachusetts Institute of Technology (MIT) are presented in this section of the chapter, since these control techniques that lack dynamic flow effect compensations are still on use. These experiments are conducted at quasi static flow conditions with zero incoming flow speeds $V_a \approx 0$ that means, flow generation with thruster towing or incoming artificial water current methods are not used.

2.2.1.1. Fixed Feed-forward Thrust Control

The most common thrust control algorithm used on UMVs is Yoerger's simple feed-forward controller which is also known as "open loop proportional control" (Yoerger et al. 1999, Roberts 2006). In this approach, the input motor current i_m is defined in Equation 2.1.

$$i_m = {k_m}^{-1}\, \alpha_1\ T_r \tag{2.1}$$

In the Equation 2.1, α_1 (Nm/N) is an experimentally determined constant, T_r (N) is desired thrust set point received from thruster allocation, and k_m (Nm/Amp) is motor torque constant. In this open loop controller, motor current specified as a linear function of the desire thrust T_d (N). The value of the torque constant α_1 can be provided by motor vendors or experimentally determinable.

In 1999, Whitecomb and Yoerger tested this controller in open water conditions (Kim 2005). During tests, sinusoidal varying thrust set points are sent to controller, and actual produced thrust is observed. Thrust control test result of fixed feed-forward thrust controller from Yoerger's study is presented in Figure 2.1.

According to Yoerger and Whitecomb, "the performance of the fixed forward thrust controller varies with thrust level". At high thrust level this controller exhibit a well-defined phase between actual and desired thrust. However at low thrust demands, controller delivered poor performance compared to other control algorithms (Yoerger et al. 1999). As it seen from Figure 2.1, controller provided a tolerable thrust tracking with a time delay.

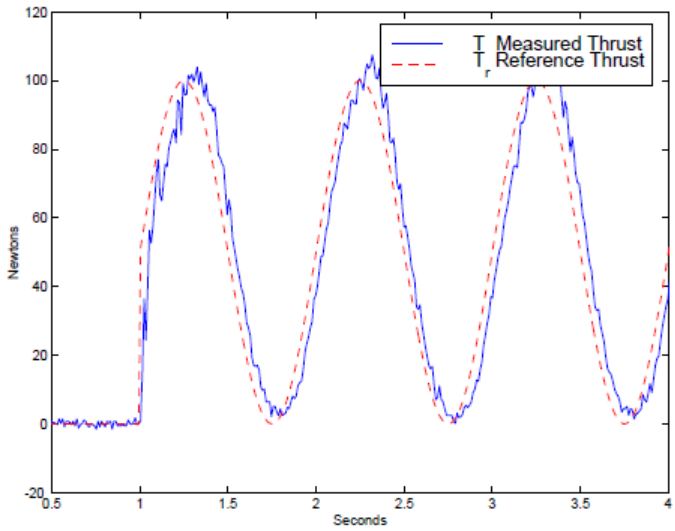

Figure 2. 1. Yoerger's fixed forward thrust control
(Source: Yoerger et al. 1999)

This controller with experimentally determined parameters is tested at zero and non-zero advance velocity conditions in this thesis study and results are discussed in Chapters 5 and 6. During the thrust control tests, this controller's performance at non-zero incoming flow conditions is found unreliable.

2.2.1.2. Feed-back Velocity Control

Different thruster low-level controllers based on velocity feedback gain are designed in past decade. Primary control objective of these controllers is maintaining

propeller velocity tracking between actual and ideal propeller rotation speeds with fast transient response. Ideal propeller rotation speed can be estimated by different methods. In Yoerger's study, ideal shaft speed is estimated by a function that includes many different parameters (Ruth 2009). Yoerger and his colleagues defined thrust force as in Equation 2.2. They assumed that, "thrust force is a quadratic function of shaft speed and a variable α_2 which includes propeller body properties" (Yoerger et al. 1999). The control parameter α_2 is given in Equation 2.3;

$$T = \alpha_2 n \lfloor n \rfloor \tag{2.2}$$

$$\alpha_2 = \rho A r^2 \eta^2 tan\, p^2 \tag{2.3}$$

In the Equations 2.2 and 2.3, η (-) is the propeller efficiency coefficient, p (m) is the pitch of the propeller, A (m^2) is the propeller area, n is the propeller shaft speed (rps) and ρ (kg/m^3) is density of the fluid.

This relation does not contain dynamic flow model but it can easily be applicable to all size and kind of propellers by changing values of parameter α_2. On the other hand like all other velocity feedback based thrust controllers, motor current i_m (A) is defined as in Equation 2.4 in Yoerger and his colleagues' controller.

$$i_m = {k_m}^{-1} \alpha_1 T_r + {k_m}^{-1} k_f (n_a - n) \tag{2.4}$$

In Equation 2.4, k_f (Nm.s/rps) is the experimentally determined motor friction coefficient, α_1 is experimentally determined constant, n is the ideal propeller shaft speed which is obtained from Equation 2.2 and n_a is the actual propeller shaft speed (rps). According to these equations, it is clearly seen that accurate control of propeller velocity error means accurate control in thrust production.

Authors indicated that "this controller do not exhibit the delay that observed in the open-loop controller's results" (Yoerger et al. 1999). Addition to this, at zero crossing of desired thrust value, these types of controllers are chattering. Since the reference propeller velocity varies as sign square root of the reference thrust propeller acceleration is infinite at zero crossing (Yoerger et al. 1999). Thrust control test results of thrust controller with feed-back velocity are presented in Figure 2.2.

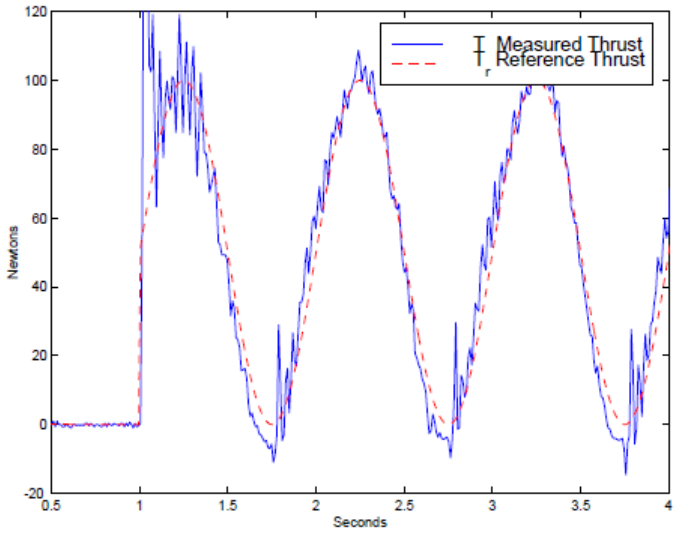

Figure 2. 2. Yoerger's feedback based controller
(Source: Yoerger et al. 1999)

Same motor current relation which is given in Equation 2.4, is used in the thrust controller designed in this thesis. Four-quadrant propeller characteristics are used in order to estimate ideal shaft speed in method developed in this thesis instead of using quadratic function relation between desired thrust force and shaft speed. Contrary to Yoerger's study, by using four-quadrant propeller mapping in estimation of ideal shaft speed, dynamic flow effect compensation is achieved in experiments conducted in work presented in this thesis.

2.2.2. Experiments at Non-zero Advance Speed

Studies with non-zero advance speed that similar to the work carried out in this thesis are presented in this section.

2.2.2.1. Four-quadrant Thrust Estimation

Reactions of marine propellers in all kind of UMV navigations are investigated by researchers in order to achieve controllers that provide efficient thrust productions. In Norwegian University of Science and Technology (NTNU), a thrust estimation scheme was proposed for marine propellers that can operate in the full four-quadrant

range of the propeller shaft speed and vehicle speed by Smogeli and his colleagues (Ruth 2009).

Scheme was formed by a nonlinear observer to estimate propeller torque and shaft speed. Four quadrant model-based torque controller was experimented in a towing tank with a real thruster. A wake screen was used to simulate wake fraction effects of vehicle's body structure. Smogeli's test set-up is depicted in Figure 2.3.

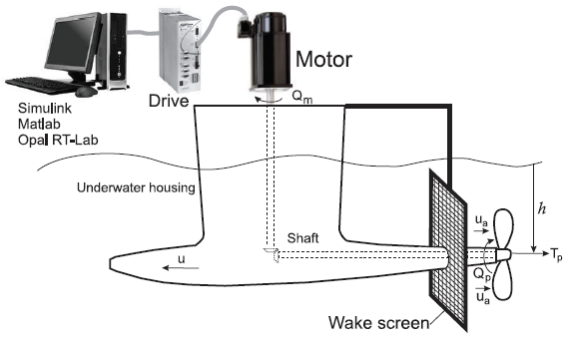

Figure 2. 3. Smogeli's four quadrant thrust estimation test-bed
(Source: Smogeli et al. 2008)

Propeller characteristics of four-quadrant UMV navigation are investigated at the range of 1 to -1 advance number J (-) for both positive and negative shaft speed. Thrust coefficient K_T, torque coefficient K_Q and efficiency η with respect to advance number J diagrams are given in Figure 2.4.

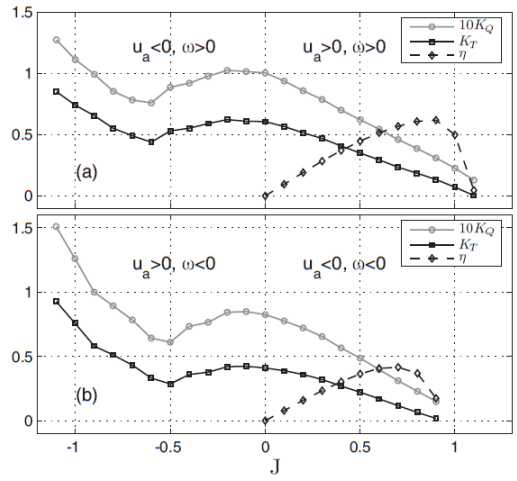

Figure 2. 4. Smogeli's four quadrant propeller characteristic investigation results
(Source: Smogeli et al. 2008)

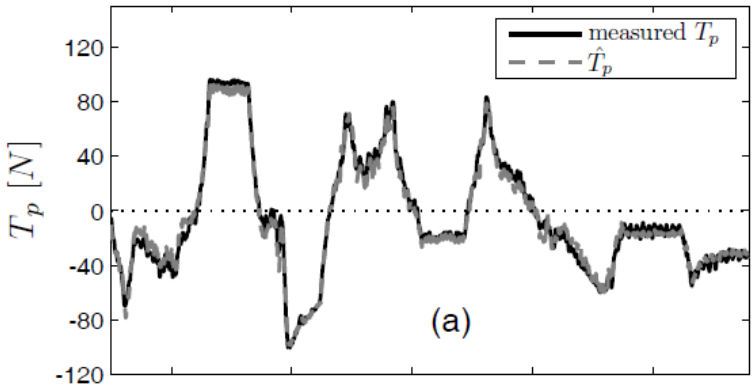

Figure 2. 5. Smogeli's four quadrant thrust estimation thrust control results (Source: Smogeli et al. 2008)

Authors indicated that "thrust controller based on torque estimation is performed well for both low and high thrust demands" (Smogeli et al. 2008). Thrust estimation result with respect to time is given in Figure 2.5. According to researchers, "this controller's performance showed that model-based thrust estimation based on four quadrant propeller characteristics can give acceptable results for UMVs that operate in dynamic flow conditions" (Smogeli et al. 2008).

2.2.2.2. Critical Advance Ratio Model

A different approach is proposed by Jin Yun Kim and his colleagues in Pohang University of Science and Technology (POSTECH) in 2005 (Kim et al. 2005). Contrary of four-quadrant model controllers, Kim's model only uses measurable states of four-quadrant navigation. They defined axial flow as a linear combination of the ambient incoming flow through propeller disc and shaft speed. In their study, thrust map is divided into three states according to state of ambient flow and propeller shaft velocity, and one of the borders of the states is defined as critical advance ratio J^*. Vague directional, anti-directional and equi-directional flow states and critical advance ratio diagrams are given in Figure 2.6 and 2.7 respectively.

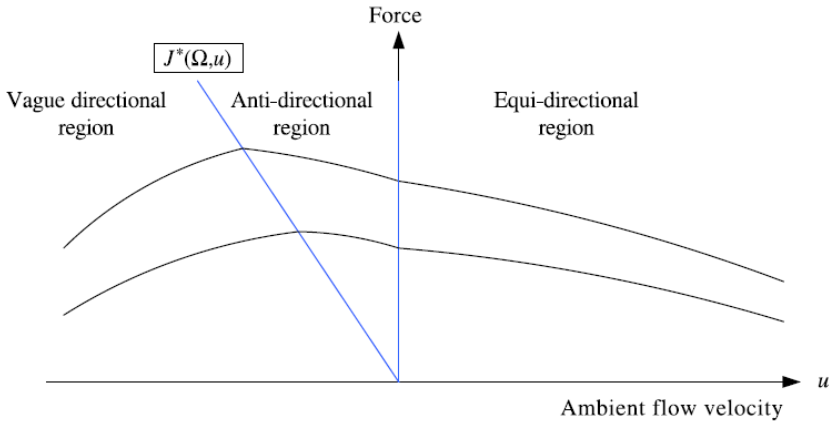

Figure 2. 6. Thrust force as a function of ambient flow velocity
(Source: Kim et al. 2005)

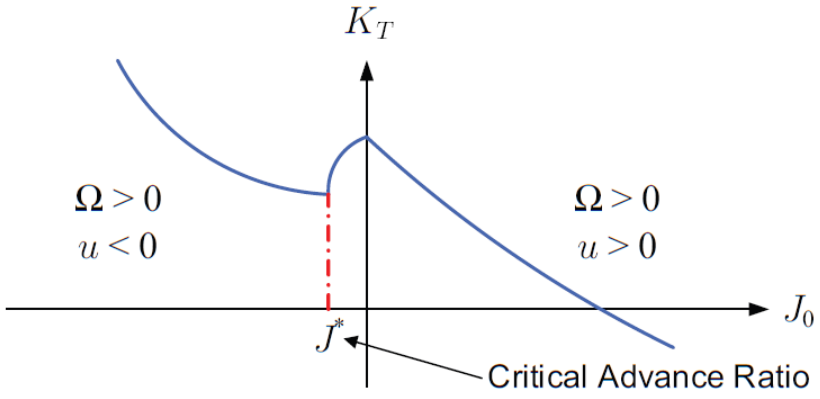

Figure 2. 7. Critical advance ratio mapping
(Source: Kim et al. 2005)

Effect of the ambient flow velocity and angle are also analyzed in Kim's study. The graph which shows ambient velocity effects over thrust force is depicted in Figure 2.8. Additionally, authors indicated that "thrust matching results between simulations with real experimental results shows excellent correlations with only ±2 N error in the entire space of thrust force under various ambient flow velocities and incoming angles" (Kim et al. 2005).

Test-bed that used in Kim's study is similar to the test bed developed in this thesis study. Instead of using towing tank, they used a static water tank with and artificial flow current to simulate the ambient flow. Test-bed is depicted in Figure 2.9.

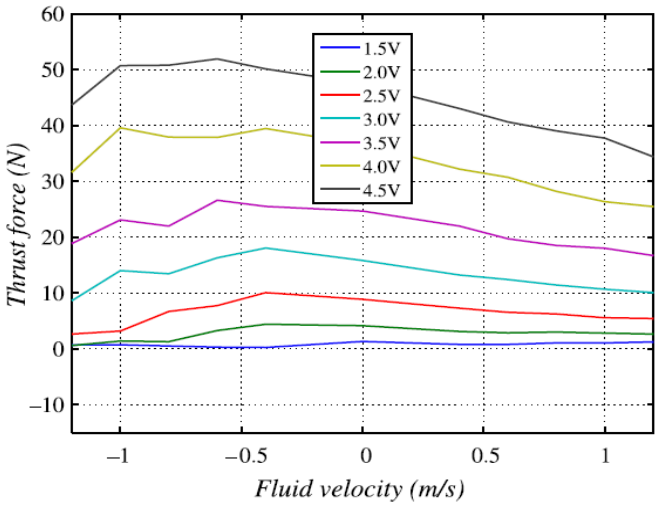

Figure 2. 8. Effects of ambient velocity over thrust force
(Source: Kim et al. 2005)

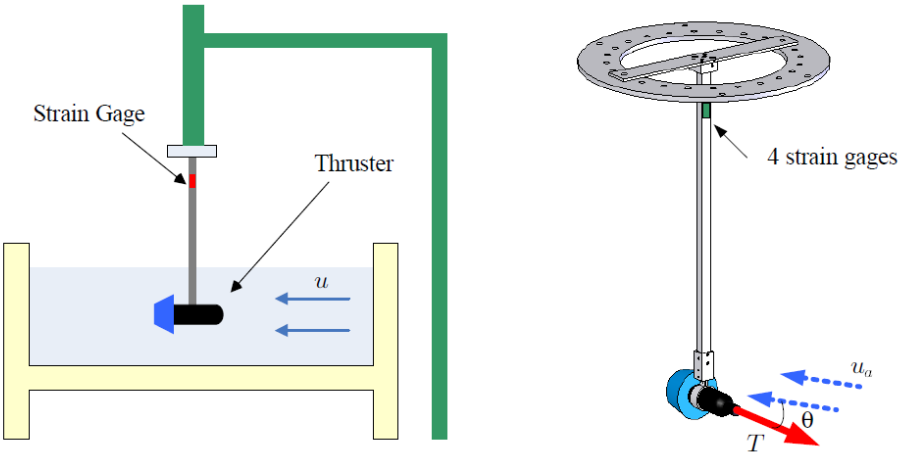

Figure 2. 9. Test bed of thrust control study with critical advance ratio model
(Source: Kim et al. 2005)

CHAPTER 3

METHODOLOGY

In this chapter, experimental test set-up and methods used in open water performance and thrust control tests are introduced. Also propeller's nominal and four-quadrant open water characteristics are presented.

3.1. Experimental Test Set-up

In general, thrust control studies and open-water tests are conducted in a long towing tanks or cavitation tunnels. Purpose of these tests is to observe the reactions of the propeller at different flow circumstances. Pumps and towing mechanisms generally are selected to create inflow water current through propeller disc area in axial direction. The effects of cavitation and ventilation can also be examined during the tests.

A 3-D computer aided design (CAD) software was used during the experimental test setup in the design steps. Experimental test setup's 3-D drawings from isometric and left views are given in Figures 3.1 and 3.2 respectively. Initial test setup geometry was changed by adding a secondary block where control thruster was attached, due to the vibration problem which is likely to occur at anti-directional flow conditions of tests.

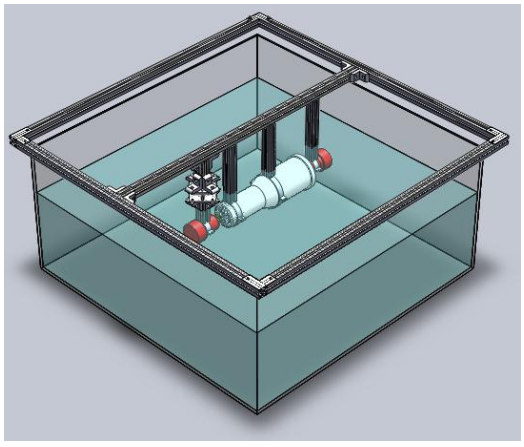

Figure 3. 1. Initial experimental test setup 3-D drawing isometric view

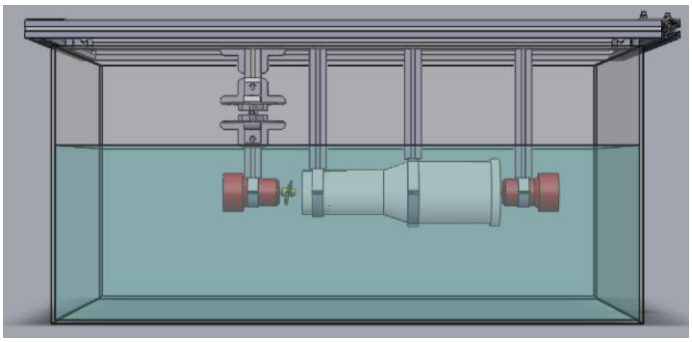

Figure 3. 2. Initial experimental test setup 3-D drawing left view

Experiments were executed by using a modified bilge pump instead of a commercial thruster, due to funding problem of the study. The pump's propeller was replaced with a 60 mm 3 bladed RC model brass propeller with unknown open water characteristics. The control thruster's pollard pull conditions were measured to be 24.4 Newton in forward and 16.6 Newton in reverse directions.

Thruster was placed in a circulating water channel with a beam where force transducer was attached. To simulate vehicle velocity effect, an artificial flow current was created by a second thruster which had a four bladed plastic propeller (80 mm diameter), an acceleration nozzle and a five cm length honeycomb layer to make the ambient flow current laminar. Layout of experimental setup is given in Figure 3.3.

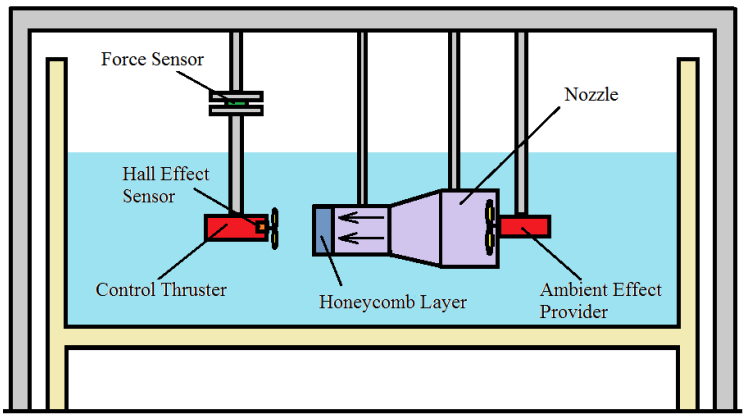

Figure 3. 3. Layout of experimental test setup

The proposed model was verified by experiments with various ambient flow velocities. During the tests, ambient flow velocity was limited between -0.304 m/s to

0.325 m/s due to the power restriction of the second thruster. To consider precisely the effects of ambient flow velocity, a real vehicle with thrusters in a long basin should be used in the experiments. However with the 1x1x0.5 meter cube tank volume, too many uncertain parameters are involved in the flow model, so experiments for arbitrary vehicle velocities instead of real velocities were done. The experimental setup and thruster allocation are depicted in Figures 3.4 and 3.5 respectively.

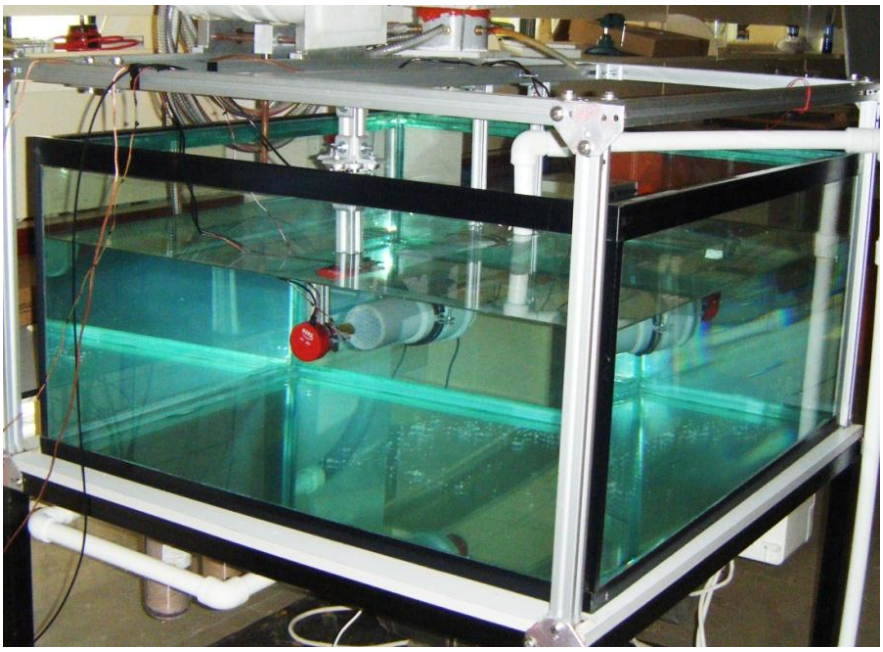

Figure 3. 4. Experimental test setup

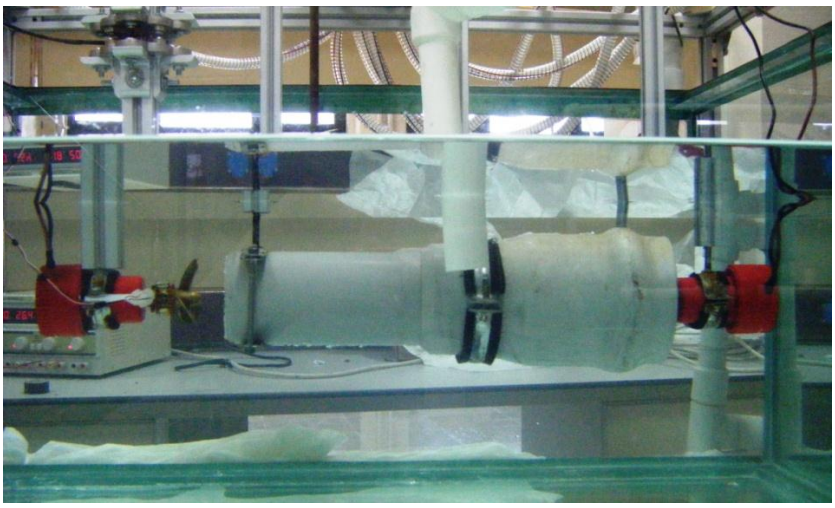

Figure 3. 5. Allocation of thrusters

Kistler® 9047B, three components miniature force sensor, was attached to the beam where the control thruster were mounted to measure thrust force. Calibration of force sensor was executed in air with known masses. The force sensor and its charge amplifier are depicted in Figures 3.6 and 3.7 respectively. Technical data of force sensor is given in Table 3.1.

Range	**Overload**	**Sensitivity**
(F_X, F_Y -10....10 kN) (F_Z -20....20 kN)	(F_X, F_Y -12....12 kN) (F_Z -24....24 kN)	(F_X, $F_Y \approx$ 8.1 pC/N) ($F_Z \approx$ 3.7 pC/N)
Rigidity	**Max. Moments**	**Weight**
(c_X, $c_Y \approx$ 600 N/µm) ($c_Z \approx$ 1400 N/µm)	(M_X, $M_Y \approx$ -200/200 Nm) ($M_Z \approx$ -120/120 Nm)	237 gr

Table 3.1. Force sensor technical data

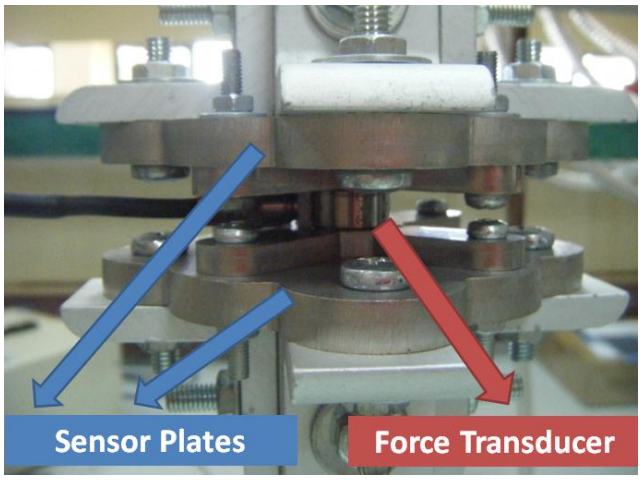

Figure 3. 6. Kistler® 9047 B three components miniature force sensor

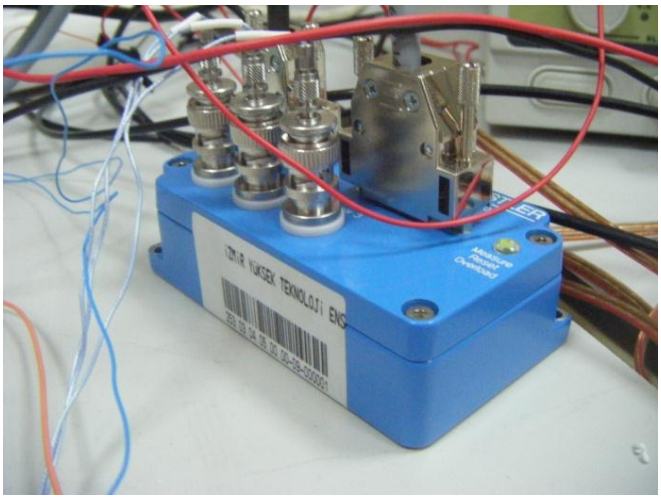

Figure 3. 7. Force sensor's charge amplifier

3.2. Measurements, Data Logging and Filtering

Thrust force data was filtered with 10 Hz second order low-pass filter in order to reduce noise on the signal. 8 channels 14 bit analog I/O, 32 bid digital I/O Humusoft® MF624 card was used as data acquisition system (DAQ). Control experiments was conducted by using Matlab SIMULINK® and Microsoft Windows Real-Time Workshop® under Microsoft Windows® operating system with 1 kHz sampling rate. For motor drivers, MAXON® LSC 30/2 4-Q-DC servo amplifier was used for each thruster.

Measurements are shown in Table 3.2 and schematic diagram of experimental data traffic is displayed in Figure 3.8. All variables in the control algorithm were logged. Some comments on the various measurements are given below;

- Propeller thrust measurement was the noisiest signal. Due to the nature of piezoelectric force sensors, surge on the water surface and vibration on the structure dramatically affected the reading of thrust.
- Shaft speed measurement was of reasonable quality and did not generate continuous signals. Due to this reason, PI or PID controller could not be used. Since Matlab/Simulink has discrete derivative function, PD control was only option available for control of velocity error.

- Drag force was measured in order to achieve real propeller thrust. Obtained thrust values were recorded with respect to the ambient flow thruster current inputs while first thruster was not working. Relation between the drag force and the advance velocity was achieved by using these data. This relation is embedded into the thrust controller code. According to the flow condition of test settings, these drag forces were added or extracted on the measured thrust value.

Parameter	Symbol	Unit	Sensor
Propeller thrust	T_a	N	Force transducer
Shaft speed	n	rps	Hall-effect sensor

Table 3. 2. Measurements in the experimental setup

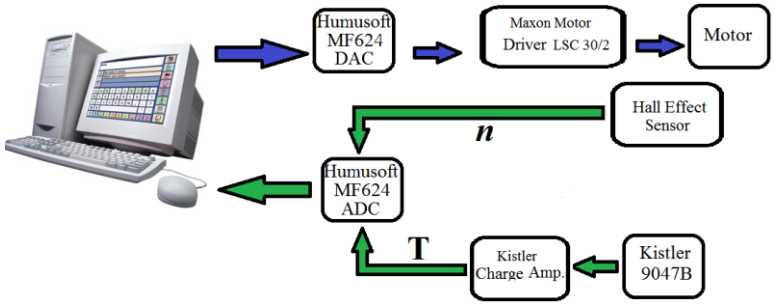

Figure 3. 8. Schematic diagram of experimental setup

3.3. Measurement of Ambient Flow Velocity

Determination of propeller characteristic is very important for accurate and precise control of a vehicle (Kim et al. 2005). Therefore measurement of ambient flow velocity which passes through propeller plane in axial direction is required. The relationship between ambient flow velocity V_a and vehicle speed u is given in Equation 3.1.

$$V_a = u\,(1-w) \tag{3.1}$$

In Equation 3.1, *w* is wake fraction coefficient which is a constant parameter that depending on vehicle's hydrodynamic property. In experiments, since there was no resistance between propeller and water flow like vehicle's hull or pod, it was assumed that the wake fraction coefficient was equal to zero and ambient flow velocity was equal to axial water velocity at nozzle's outlet.

Various methods of measurement of ambient flow velocity have been used in literature, the most common ones were with pitot tubes and acoustic doppler velocity meters.

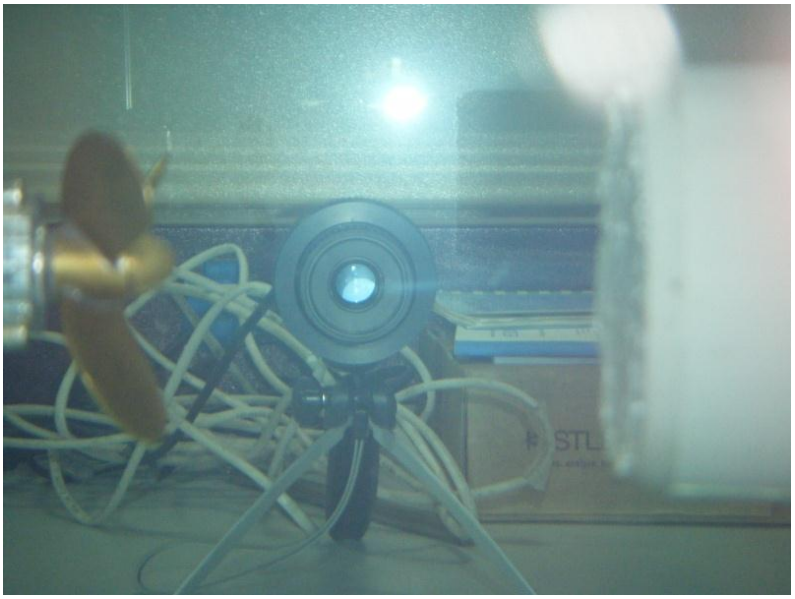

Figure 3. 9. Particles monitoring with high speed camera

In this study, particles monitoring with high speed camera method was used. A picture form this process is presented in Figure 3.9. Polystyrene particles which had a density value close to the density of water, were added into the ambient flow current that was provided by the ambient-flow thruster's propulsion. Particle movements were observed by Pulnix® TM 1020 15CL high speed camera and the velocities were recorded at the outlet of the acceleration nozzle. Two sample pictures from particle monitoring tests are given in Figure 3.10. These tests were conducted ten times and results were averaged for each ampere value of the second thruster. Relationship between ambient-flow thruster's ampere value and ambient velocity was achieved by these tests. Ambient flow velocity by ambient-flow thruster's current diagram is given

in Figure 3.11. In thrust control test, relation between motor current and flow velocity was assumed to be linear and this function is embedded into controller Simulink code.

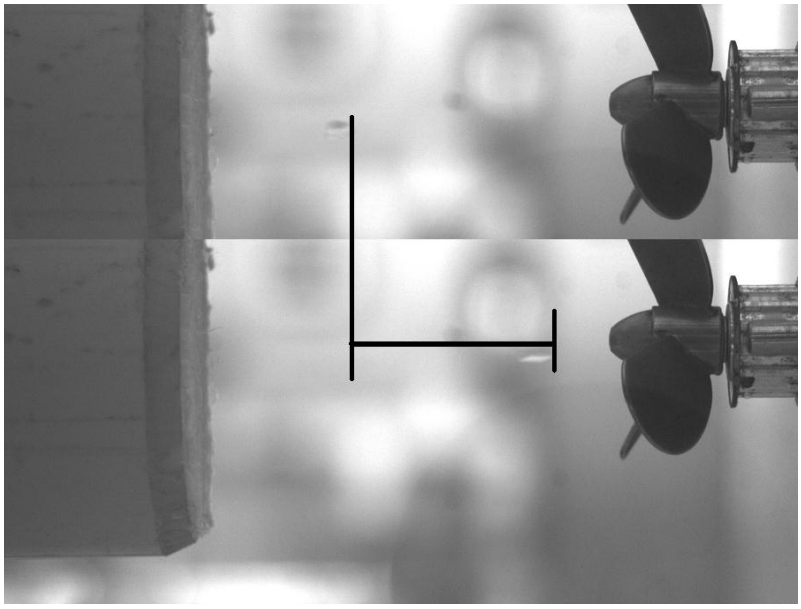

(a)

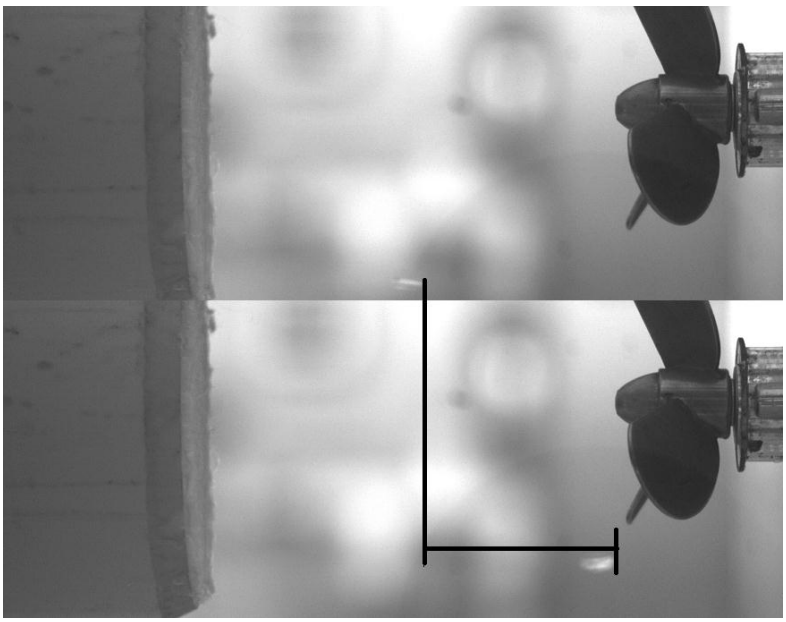

(b)

Figure 3. 10. Polystyrene particles movement (a: 0.1855 m/s at 1A thruster current, b: 0.1513 m/s at 0.8A thruster current)

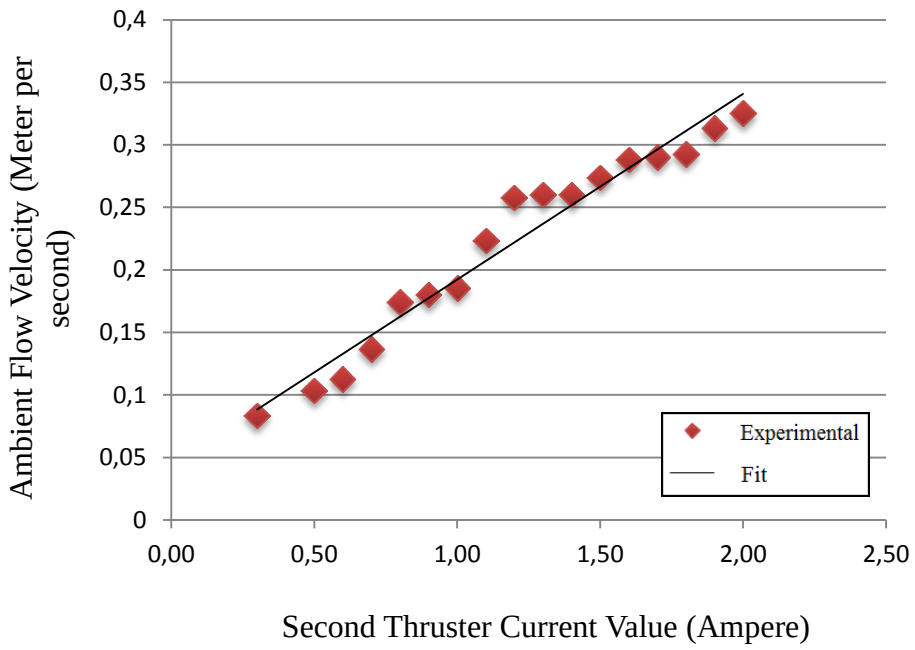

Figure 3. 11. Ambient flow velocity – ambient effect thruster current diagram

3.4. Measurement of Propeller Shaft Speed

UGN 3113 Hall Effect switch is used to measure propeller shaft speed since bilge pumps do not have encoders. Propeller shaft is extended with a coupling which carries two equally spaced neodymium magnets due to the inertia problem. The output signals of the Hall Effect switch are processed by a Simulink code and real-time shaft speed is processed. Hall Effect switch's technical data is presented in Table 3.3. Shaft speed measurement mechanism is depicted in Figure 3.12.

Supply Voltage	**Magnetic Flux Density**
4.7....25 V	Unlimited
Continuous Output Current	**Operating Temperature Range**
25 mA	-25 C°..... 85 C°

Table 3. 3. Hall Effect switch technical data

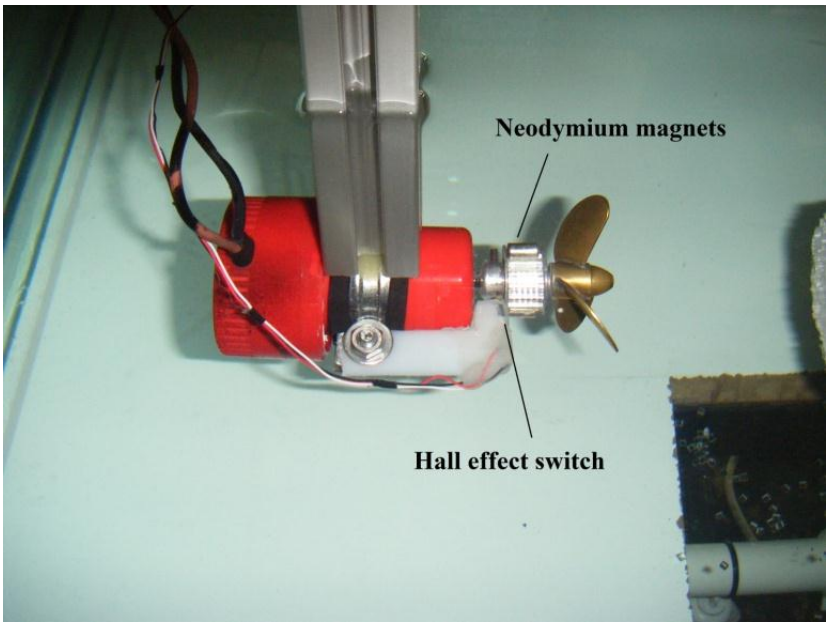

Figure 3. 12. Shaft speed measurement

3.5. Open-Water Tests

Actual thrust T_a, is influenced by many parameters; such as incoming flow velocity and angle and submergence. T_a is generally formulated as functions of propeller shaft speed n in revolution per second (rps), time varying states x_p (advance velocity, submergence etc.), and fixed thruster parameters θ_p (propeller diameter, propeller pitch, geometry etc.) (Smogeli et al. 2005). Actual thrust is defined in Equation 3.2.

$$T_a = f_T(n, x_{p,} \theta_p) \tag{3.2}$$

The function f_T may include thrust losses due to in-line transverse velocity fluctuations, ventilation, in and out water effects, thruster-thruster interaction and dynamic flow effects (Smogeli 2008).

The quasi-static relationships between T_a, Q_a, n, propeller diameter D, and density of water ρ are given in Equations 3.3 and 3.4.

$$T_a = f_T(\ldots) = sign\,(n)\, K_T\, \rho\, D^4\, n^2 \tag{3.3}$$

$$Q_a = f_Q(\ldots) = sign\,(n)\, K_Q \rho\, D^5\, n^2 \tag{3.4}$$

K_T and K_Q are the thrust and torque coefficients, where the thrust and torque losses are accounted for. In general thrust and torque coefficients are expressed in a similar manner as actual thrust in Equations 3.3 and 3.4 (Smogeli et al. 2005) by Equation 3.5 and 3.6 respectively.

$$K_T = K_T(n, x_p, \theta_p) = \frac{T_a}{sign(n)\,\rho\, D^4 n^2} \tag{3.5}$$

$$K_Q = K_Q(n, x_p, \theta_p) = \frac{Q}{sign(n)\,\rho\, D^5 n^2} \tag{3.6}$$

The open-water parameters, thrust coefficient and torque coefficients, are experimentally determined by so-called open-water tests that are usually performed in cavitation tunnels or a towing tank. For specific propeller geometry $K_{T\,(J)}$ is usually given as function of advance number (J_a) which is presented in Equation 3.7.

$$J_a = \frac{V_a}{n\,D} \tag{3.7}$$

In Equation 3.7, V_a is the propeller advance velocity, D (m) is the diameter of propeller and n (rps) is the propeller shaft speed.

Open water efficiency η_o, which is given in Equation 3.8, is described as ratio of produced power to consumed power for the propeller (Smogeli et al. 2005).

$$\eta_o = \frac{V_a T_a}{2\,\Pi\, n\, Q_a} = \frac{J_a K_T}{K_Q 2\,\Pi} \tag{3.8}$$

These non-dimensional parameters are used to display open-water performance of a propeller. Test procedure that is applied to obtain open-water characteristic of three-bladed test propeller is outlined as follows:

- The range of measurement should cover tested propeller operating range in terms of advance number J. Range of -1 to 1 is selected for the tests.
- In general the circulating water, V_a, kept constant while the propeller rate of rotation is varied.

- In each run, the ambient flow velocity V_a, propeller rotation n, thrust force T_a, thruster current and voltages are recorded.
- The non-dimensional coefficients are obtained analyzing the test results and they are plotted for every different flow scenario in order to complete four-quadrant propeller operation map.

3.5.1. Nominal Characteristics

The nominal thrust T_n, torque Q_n and power P_n are ideal values when no thrust losses are present. Especially, in thruster control for station-keeping operations, estimated nominal thrust and torque coefficients are usually chosen as control coefficients, because actual advance velocity is unknown for controller. Doppler Logs or GPS systems may be used to give estimates of advance velocity but these measurements are needed to be precise enough and in real-time for inclusion in the low-level thruster controller. If the propeller characteristics are known, improved controller performance may be achieved by estimating advance velocity, V_a. The advance velocity can be estimated by using known vehicle speed u and the relation that includes hull wake fraction coefficient.

In the experiments, nominal thrust is calculated at zero advance velocity condition. In spite of zero advance speed, propeller is still doing work by accelerating water through the propeller disc. From momentum theory (Duran et al. 1963) the mean water velocity, V_p , through the propeller disc is given for $V_a = 0$ by Equation 3.9.

$$V_p = 0.5 \; sign\,(T_n) \sqrt{\frac{2\,T_n}{\rho A_P}} \tag{3.9}$$

In Equation 3.9, T_n is the nominal thrust, ρ is the density of water and A_p is the propeller disk area. According to this data, nominal thrust value – shaft speed, mean water velocity – shaft speed and propeller open water efficiency – advance number in nominal condition diagrams are given in Figures 3.13, 3.14 and 3.15 respectively. Also, relation between the nominal thrust coefficient and the advance number is displayed in Figure 3.16.

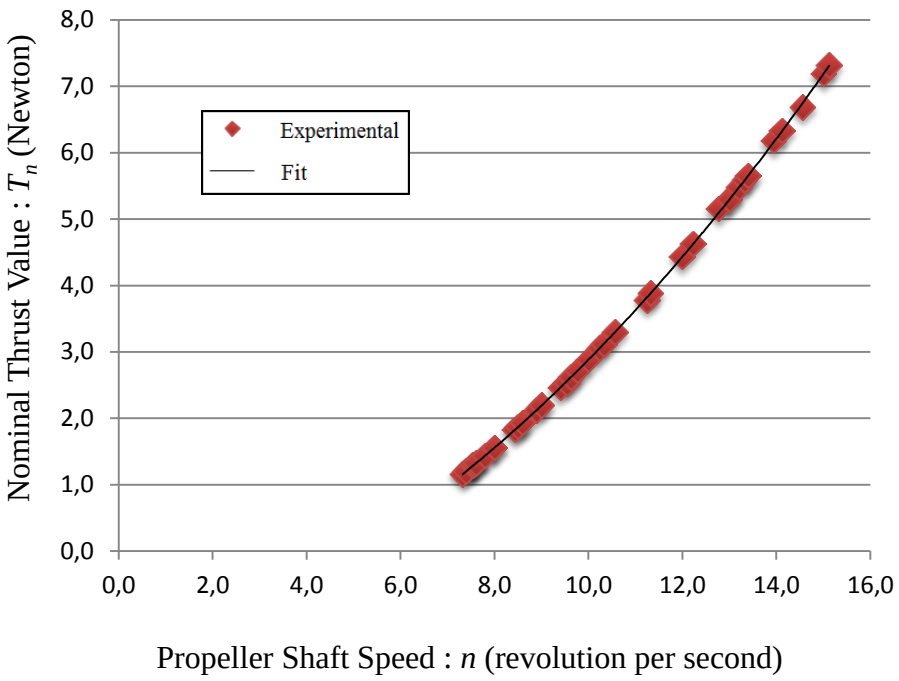

Figure 3. 13. Nominal thrust value – propeller shaft speed diagram

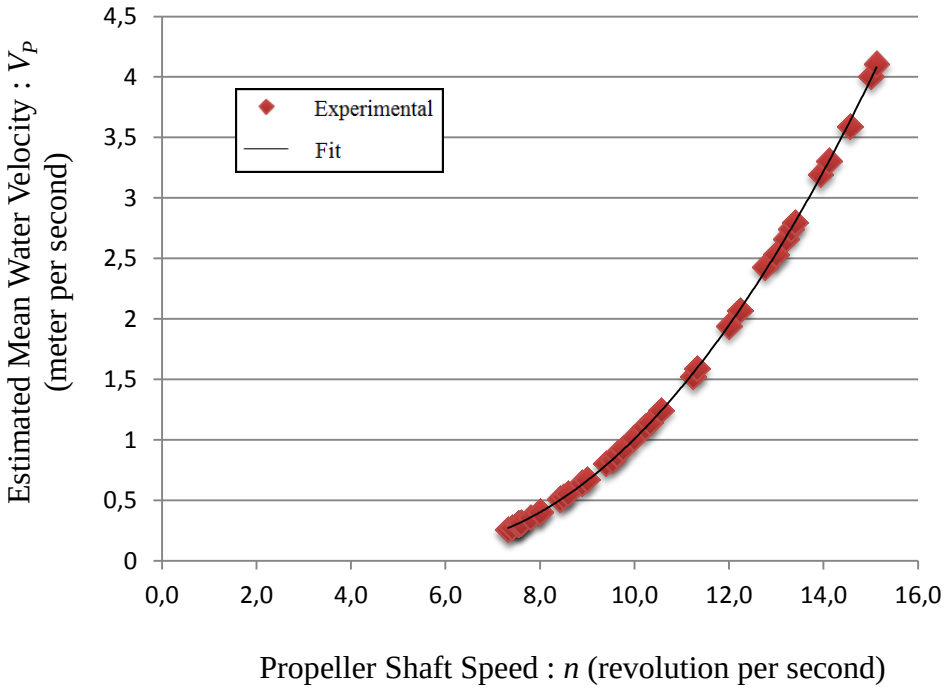

Figure 3. 14. Estimated mean water velocity – propeller shaft speed diagram

Linear fits were applied to the data for K_T-J and T_n-n, a third order fit was used for η-J and a second order fit was used for V_p-n relations.

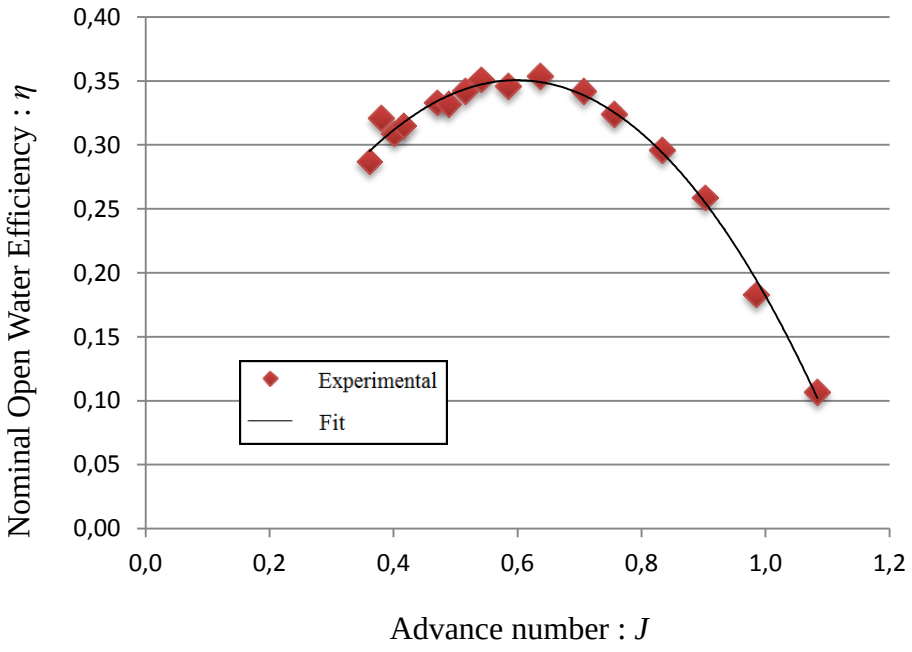

Figure 3. 15. Nominal open water efficiency – advance number diagram

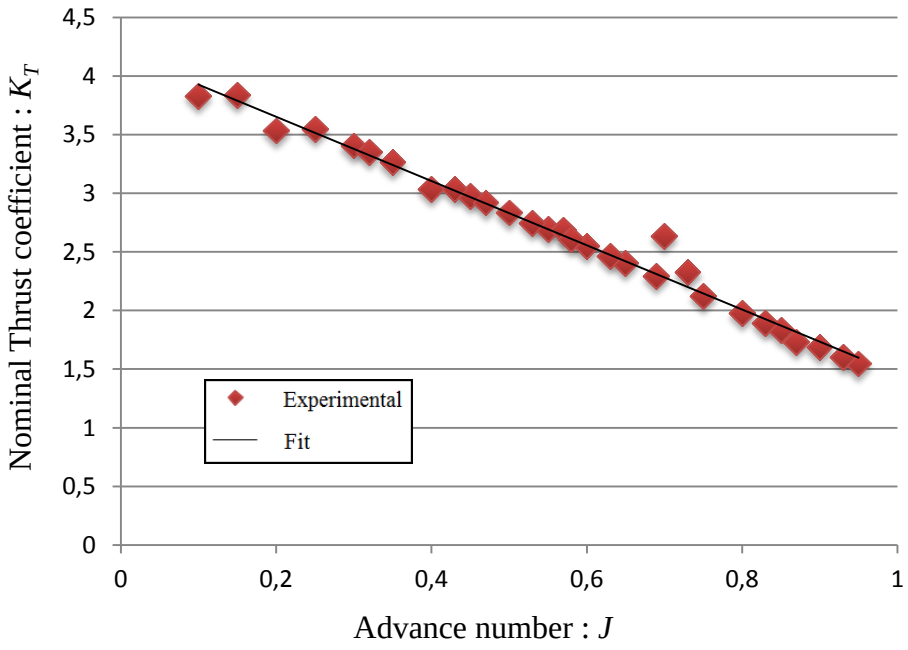

Figure 3. 16. Nominal thrust coefficient vs advance number diagram

3.5.2. Four-Quadrant Propeller Characteristics

The controllers based on models which include only nominal characteristics of propellers provide inaccurate thrust tracking results at flow conditions that differ from quasi-static navigations. In this study, the four-quadrant propeller characteristics were determined. The results that are found in these tests were embedded into the controller code to estimate correct values of rotational propeller speed required for a specific thrust demand and navigation condition. Four-quadrant operations of a propeller are shown in Table 3.4.

	1st	**2nd**	**3rd**	**4th**
n	≥ 0	≥ 0	< 0	< 0
V_a	≥ 0	< 0	≥ 0	< 0

Table 3. 4. The four quadrant operations of a propeller

3.5.2.1. First-Quadrant Characteristics

Data were collected at inflow speed of 0.301 m/s and 0.325 m/s during positive advance speed and positive shaft speed operation condition. The rotation rate was varied from 600 RPM to 1100 RPM for each inflow speed. Thrust and current were averaged over test intervals for at least 15 seconds. Each test was conducted four times and the results were averaged. Data were non-dimensionalized to produce thrust coefficient K_T for each flow conditions. Operation condition scheme is depicted in Figure 3.17. A linear fit was applied to relation of $K_T - J$, which is given in Figure 3.18.

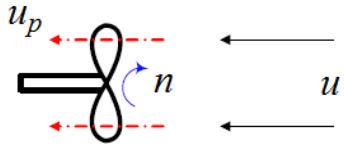

Figure 3. 17. Positive advance speed & shaft speed operation condition

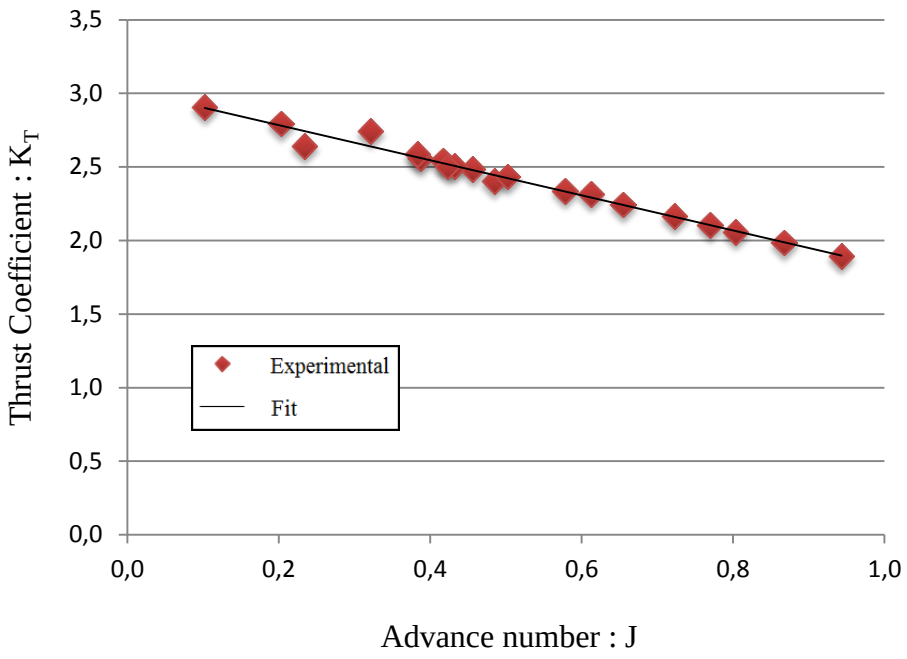

Figure 3. 18. K_T – J relation at positive advance speed & positive shaft speed

3.5.2.2. Second-Quadrant Characteristics

Thruster position was changed due to design limitation, in negative advance speed conditions. Since initial experimental set-up configuration was designed to create artificial water current which was sent through propeller suction side, thruster position was reversed in order to simulate negative advance velocity. Operation condition and flow directions are presented in Figure 3.19.

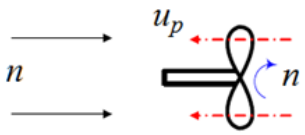

Figure 3. 19. Negative advance speed & positive shaft speed operation condition

Data were collected at the inflow speeds of -0.103 m/s and -0.302 m/s during in this quadrant tests. The rotation rate of propeller was varied from 630 RPM to 1140 RPM for each inflow speed. Thrust and current values were averaged over test intervals

for at least 15 seconds. Each test was conducted four times and the results were averaged. Data was non-dimensionalized to produce thrust coefficient K_T for each flow conditions. A third-order fit was applied to relation of $K_T - J$ for this operation. Thruster allocation of second-quadrant open-water tests is presented in Figure 3.20 and thrust coefficient with respect to advance number diagram is given in Figure 3.21.

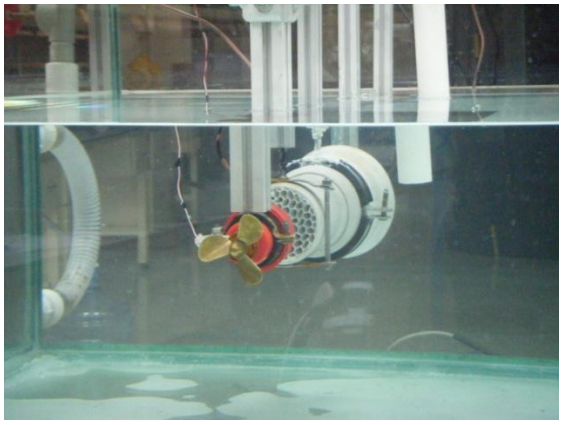

Figure 3. 20. Thruster allocation for negative advance speed tests

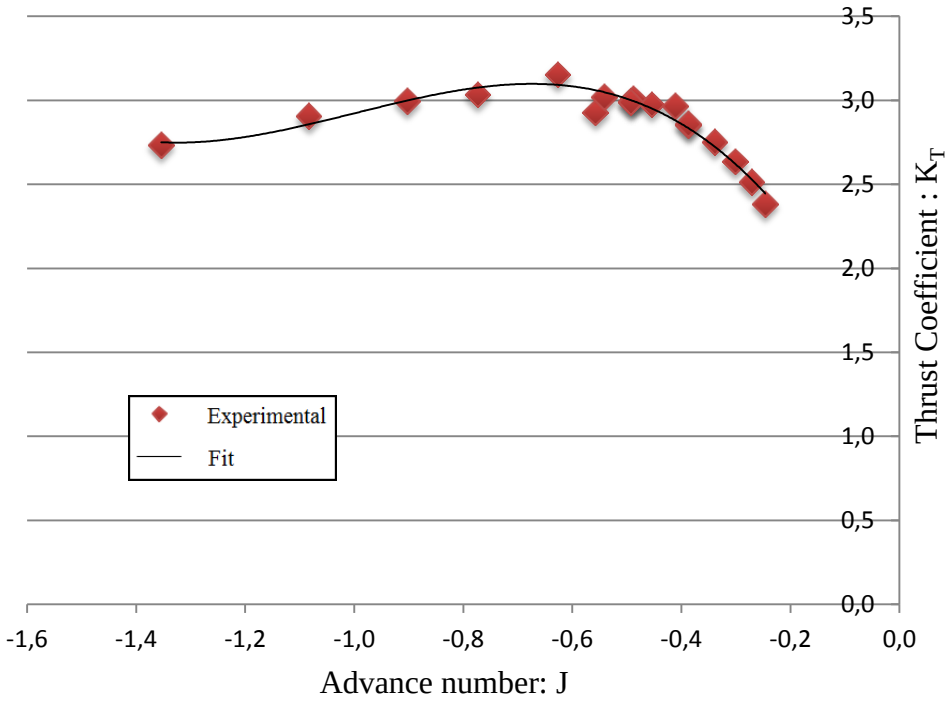

Figure 3. 21. K_T – J relation at negative advance speed & positive shaft speed

3.5.2.3. Third-Quadrant Characteristics

Data were collected at the same inflow speeds as in the first-quadrant tests. The rotation rate of propeller was varied from -630 RPM to -1140 RPM for each inflow speed. Thrust and current were averaged over test intervals for at least 15 seconds. Each test was conducted four times and the results were averaged. Data was non-dimensionalized to produce thrust coefficient K_T for each flow conditions. To achieve relation between K_T and J, third-order fit were applied to data. Operation condition scheme is depicted in Figure 3.22. A linear-fit was applied to relation of $K_T - J$ which is illustrated in figure 3.23.

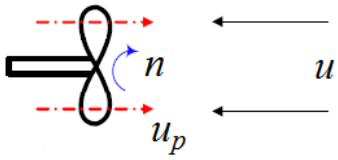

Figure 3. 22. Positive advance speed & negative propeller shaft speed operation condition

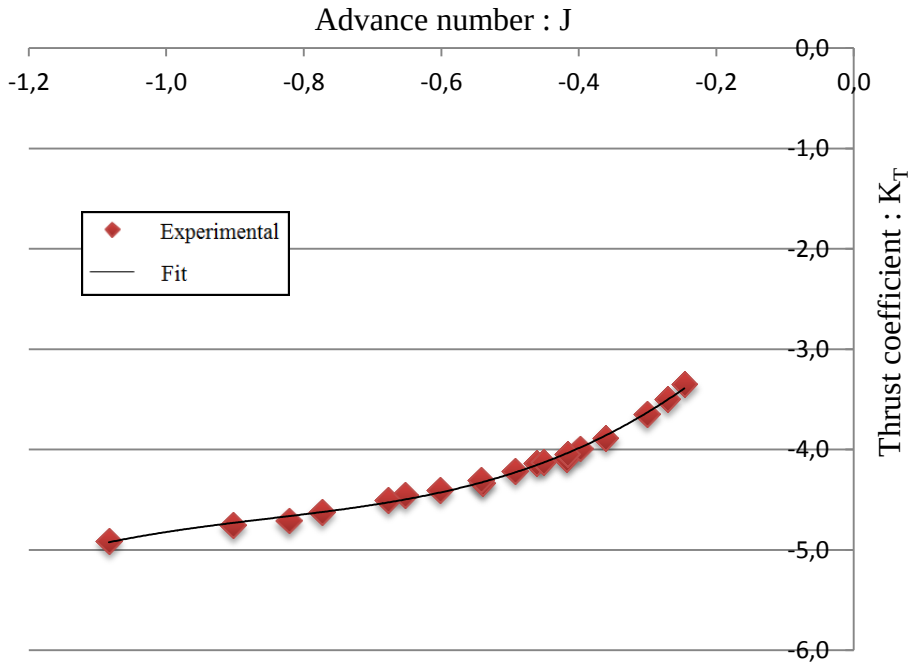

Figure 3. 23. K_T – J relation at positive advance speed & negative shaft speed

3.5.2.4. Fourth-Quadrant Characteristics

In negative advance speed and negative shaft speed tests, data were collected at the same inflow speeds as it was for the second-quadrant tests. The rotation rate of propeller was varied from -630 RPM to -1140 RPM for each inflow speed. Thrust and current were averaged over test intervals for at least 15 seconds. Each test was conducted four times and the results were averaged. Data was non-dimensionalized to produce thrust coefficient K_T for each flow conditions. A linear-fit was applied to relation of $K_T - J$ for this operation which is given in Figure 3.25, flow directions is depicted in Figure 3.24.

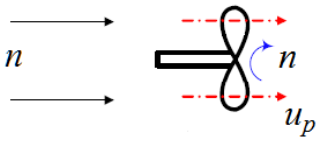

Figure 3. 24. Negative advance speed & reverse thrust operation condition

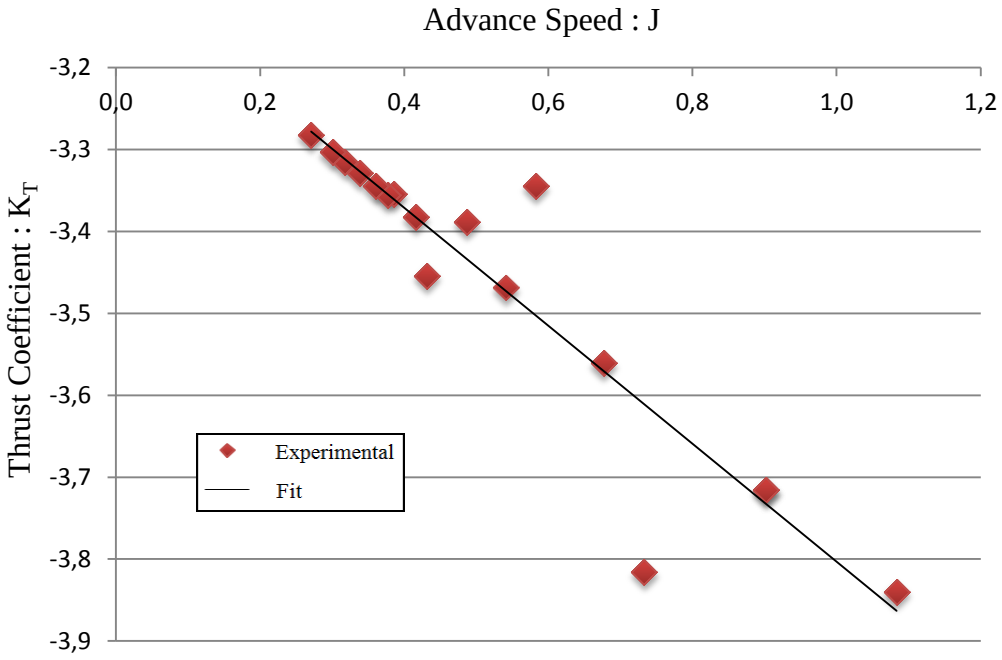

Figure 3. 25. K_T – J relation at negative advance speed & negative shaft speed

CHAPTER 4

THRUST CONTROLLER

During normal operation conditions, a low-level thrust controller was developed to track the desired thrust. For a FPP, when actual thrust is unknown, thrust was produced by different ways such as, shaft speed feedback controller, torque feedback controller, power feedback controller and hybrid combinations of these controllers. In this study, the thrust control system was complemented with a velocity feedback, to control the thrust produced by an un-ducted FPP driven by an electrical motor.

4.1. Constraints

In this study, it is assumed that only shaft speed n and velocity of vehicle u is available for measurement. The proposed controller is mainly aimed to be used at low-thrust demands for low-speed operations to be accomplished with electrically driven FPP. Variable parameters such as submergence, thrust, power and torque can also be added as a control objective in this controller concept.

The control algorithm is formulated by making use of propeller diameter D, thrust coefficient K_T and advance number J values, incoming flow velocity V_a and propeller shaft speed n.

4.2. Control Objectives

Waves, ocean currents and vessel motions induce a time varying velocity field around propeller. This may be decomposed to an in-line component and transverse component (Smogeli 2008). In-line component gives rise to the change in the advance velocity V_a and advance number J. With a time varying J, the operating point is moving on the K_T-J curves. Therefore these changes induce fluctuations in thrust, torque and power even for a fixed shaft speed n.

The goal of the controller is to make the actual thrust, T_a, to track desired thrust T_d in dynamic operation conditions with time varying in-flow velocities. Other goals for different studies may be as important as tracking demanded thrust set point T_d, e.g. limiting power oscillations, optimizing power consumption and reducing mechanical wear and tear. In this study, the following performance criteria are considered.

- Thrust production in the existence of disturbance
- Good responses in all four different types of axial flow scenarios
- Robust performance

4.3. Thruster Control Structure

In the controller structure, the desired thrust, T_d, from thrust allocation or autonomous path planner is sent to the thruster control scheme, which includes thruster open-loop control and feedback velocity error. Thruster control scheme calculates required motor current in order to reach desired thrust at current operational advance number J with the help of data which are acquired from propeller characteristic blocks. The propeller characteristic blocks are used to calculate the ideal shaft speed for current operation condition and thrust demand. The control structure is depicted in Figure 4.1.

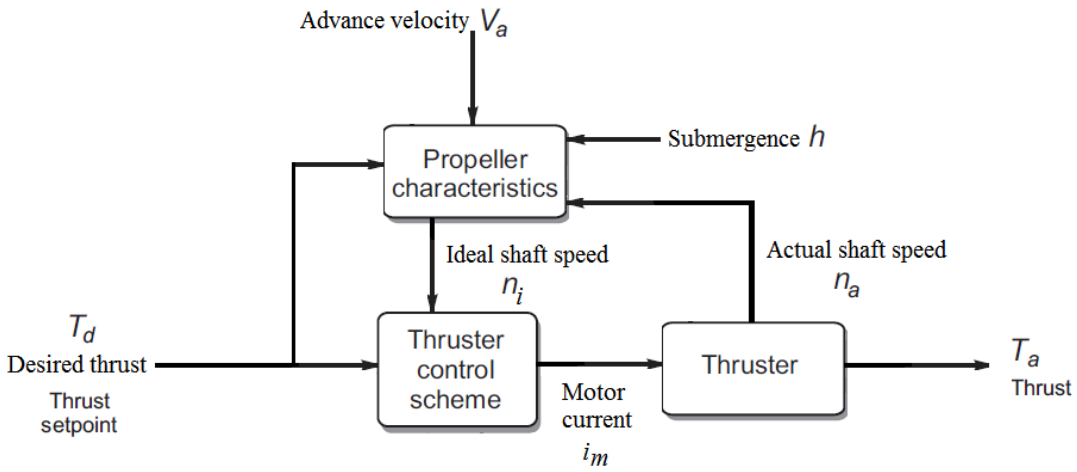

Figure 4. 1. Thrust controller structure

4.3.1. Propeller Characteristics Block

Thrust control schemes are based on the thrust, torque, velocity and power relationship. In the experimental tests, propeller diameter D and density of water ρ is assumed to be known and constant. Additionally, actual shaft speed n_a, vehicle speed u (assumed to be equal to incoming flow velocity V_a) and desired thrust demand T_d is assumed to be obtainable from vehicle's higher-level controller or thrust allocation system.

Since the controller has a velocity feed-back based control algorithm, the velocity tracking requires the values of the calculated ideal shaft speed and the measured actual shaft speed. In the propeller characteristics section of thruster controller, ideal shaft speed, n_i, which is required for acceptable trust tracking accuracy, is calculated. Propeller characteristics controller blocks are given in Figure 4.2.

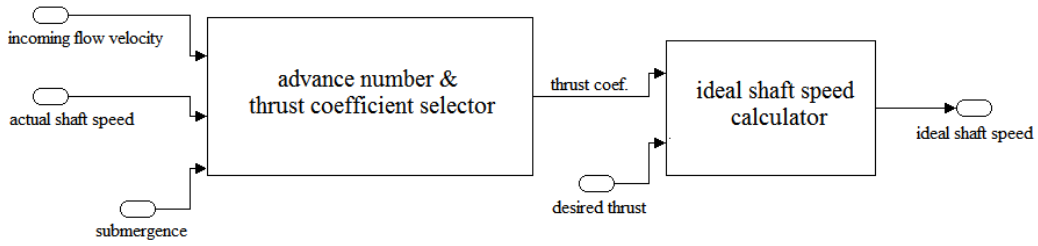

Figure 4. 2. Controller's propeller characteristics blocks

4.3.1.1. Selection of Advance Number J and Thrust Coefficient K_T

In control process, propeller characteristics block uses vehicle speed which is assumed to be equal to incoming flow velocity, actual shaft speed and density of water that depends on the environment and depth of operation, in order to calculate current operational advance number J. During advance number selection process, determination of the direction of incoming flow and propeller rotation direction are crucial to determine the sign of J. In four-quadrant operations, positive thrust and positive vehicle movement direction condition and negative thrust and negative vehicle movement direction condition give positive advance number. However, the advance number is negative for the second and third quadrant conditions. Propeller characteristics'

condition selector block is used, to determine the correct quadrant of propeller operation. This block monitors sign of the motor current and vehicle speed that are taken from vehicle's high level controllers. If sign of motor current I_m and vehicle velocity u values are both positive, selector chooses first quadrant operation, if they are both negative, then it chooses forth quadrant. Negative vehicle speed u - positive motor current I_m condition is defined as second quadrant, positive vehicle speed u – negative motor current I_m condition is defined as third quadrant.

When correct quadrant is determined controller calculates the advance number J by using Equation 3.6 and sends this number to the thrust coefficient selection part. In this thrust coefficient selection block, thrust coefficient K_T is chosen from the J-K_T graphs that was already found and embedded into the controller algorithm. Advance number and thrust coefficient selection blocks are given in Figure 4.3.

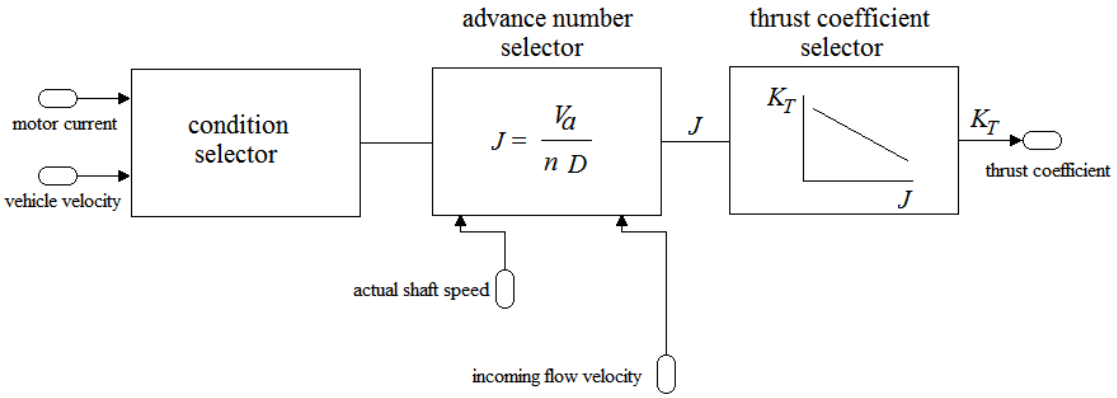

Figure 4. 3. Advance number and thrust coefficient selection blocks

4.3.1.2. Ideal Shaft Speed Calculation and Velocity Error Tracking

In order to calculate ideal shaft speed, thrust coefficient and propeller shaft speed relation which is given in Equation 3.5 are used. Since desired thrust, T_d, propeller diameter D and density of water ρ are known, ideal shaft speed n_i can be determined.

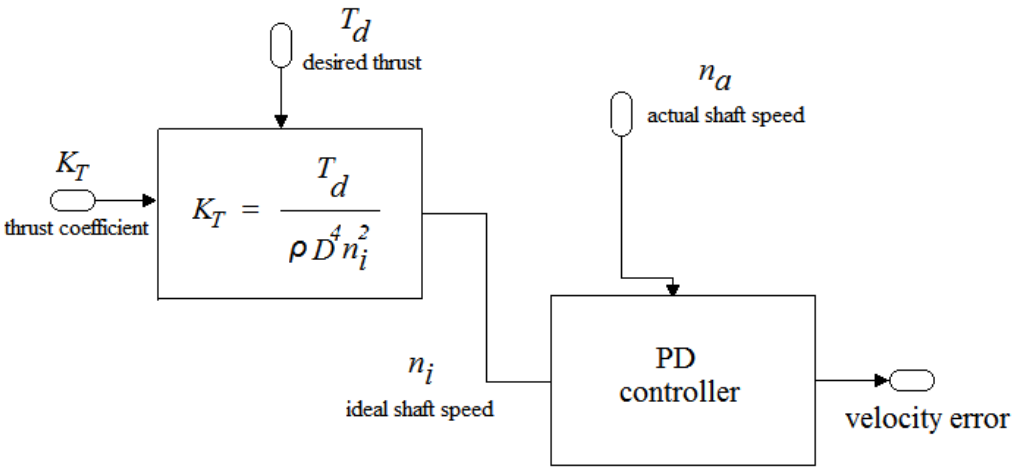

Figure 4. 4. Velocity error tracking

Ideal and actual propeller shaft speed difference is defined as velocity error e_v. However this error is not added into the core controller directly.

During the thrust control studies with the experimental test-setup, thrust fluctuations and big overshoots were observed with controller that uses a proportional controller with proportional gain equal to one. To achieve fastest possible velocity tracking without thrust fluctuations while maintaining the stability, a PD controller is employed. The PD controller for velocity tracking smoothened the error e_v, convergence to zero.

4.3.2. Thruster Control Scheme

The thrust control scheme is developed, based on Whitecomb and Yoerger's (1999) feed-back thrust controller. In the designed controller, thrust control scheme is divided into two parts. First part is commonly used in conventional open-loop controller which uses nominal thrust value – motor current match-up in order to calculate nominal output current. Other part is propeller velocity feedback controller that reduces the thrust tracking errors by reducing the velocity tracking error. The velocity error fed into the PD controller (velocity feed-back controller) is calculated by comparing the ideal shaft speed information gathered from the four quadrant propeller characteristics blocks and the measured shaft speed. Then the closed-loop PD controller is applied to decrease

the velocity errors rapidly and stably with respect to the design criteria. Thrust control structure is given in Figure 4.5.

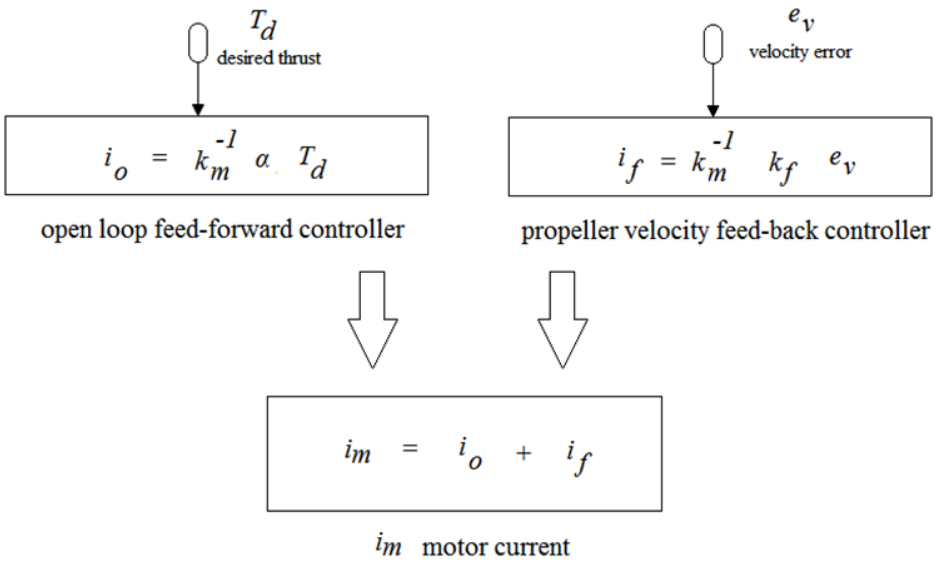

Figure 4. 5. Thrust control scheme

Controller calculates motor current i_m by adding propeller velocity feedback current i_f to open-loop feed-forward current i_o, as it is presented in Figure 4.5. This algorithm is used in Whitecomb and Yoerger (et al. 1999) feed-back based thrust controller. In spite of similarity between two studies, the controller designed in this thesis is different from their study in estimation of velocity error. In the designed control, the velocity error estimation depends on four-quadrant model-based propeller characteristics, while Whitecomb and Yoerger's controller only specifies thrust as a function of propeller rotational velocity.

4.3.2.1. Open Loop Feed-Forward Controller

In fixed feed-forward thrust controller also known as simple open-loop proportional controller in literature, output current is defined as in Equation 4.1.

$$i_o = k_m^{-1} \alpha T_d \tag{4.1}$$

In Equation 4.1, α is an experimentally determined constant and k_m is the motor torque constant. In this controller part, output current specified as linear function of the desired thrust T_d. Value of the motor torque constant k_m and α constant are experimentally determined from nominal open-water tests. Note that, constant α value is different for forward and reverse thrust demand conditions.

4.3.2.2. Propeller Velocity Feed-Back Gain

Similar to Whitecomb and Yoerger's (et al. 1999) feedback based thrust controller, a feed-back velocity controller is used to tune motor current in order to maintain accuracy on actual-ideal propeller shaft speed tracking. In literature, the current command for propeller velocity feed-back controller is defined as in Equation 4.2.

$$i_f = k_m^{-1} k_f e_v \tag{4.2}$$

In Equation 4.2, k_f is an experimentally determined friction constant, k_m is the motor torque constant and e_v is the velocity feed-back output (torque command).

With the propeller velocity feed-back torque command, actual propeller shaft speed was able to track the ideal shaft speed at all flow circumstances. Value of k_m is determined from open-water test and the friction constant k_f empirically tuned for the fastest possible velocity tracking in thrust control trials.

CHAPTER 5

THRUST CONTROL TEST RESULTS AND DISCUSSION

Experiments with a propeller based electrical thruster have been carried out in the Fluid Mechanics Laboratory in İzmir Institute of Technology, in order to test and validate the proposed controller. Experimental test setup and controller parameters are described in section 5.1 and 5.2, followed by quasi-static thrust control tests in section 5.3 and dynamic thrust control tests in section 5.4.

5.1. Experimental Test Setup Parameters

Test basin was 1m long, 1m wide and 0.5m deep. The tested propeller was 60mm diameter *D* conventional three bladed RC boat propeller and used un-ducted in all tests. The submergence of propeller *h* was kept constant and 275mm. Length *d* between output of nozzle and propeller surface was 80mm for positive advance velocity test and 135mm for negative advance velocity tests. The density of water ρ was assumed to be homogeny and 1024 kg/m^3. Linear relation between ambient effect provider thruster's current value and water velocity at output of nozzle was used in order to measure advance velocity of artificial water current. A sketch of the experimental setup is illustrated in Figure 5.1.

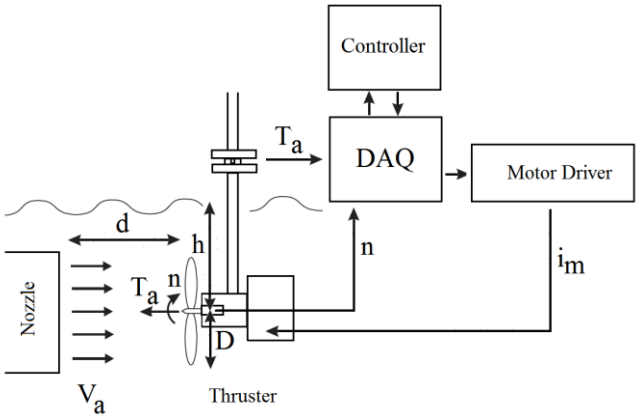

Figure 5. 1. Experimental setup parameters

5.2. Controller Parameters

Basic control parameters were chosen as in Table 6.1. Notice that all the basic controller parameters except α constant and friction coefficient k_f were kept equal for both tests for positive and negative thrust demand conditions.

α forward	α reverse	k_f forward	k_f reverse
2.18656 (Nm/N)	3.02342 (Nm/N)	-0.03265 (Nm/A)	-0.02983 (Nm/A)

K_p proportional gain	t_d differential time
0.2	0.05s

Table 5. 1. Basic controller parameters used in experiments

5.3. Quasi-static Thrust Control Tests

Advance velocity was kept constant and zero, desired thrust command was selected as to be time varying custom signal in quasi-static thrust control tests. During these tests, only open-loop feed-forward thrust controller which considered the relation between motor current and nominal thrust values, was used. Tests were lasted for 60 seconds and thrust values were recorded. Quasi-static thrust control test result is given in Figure 5.2.

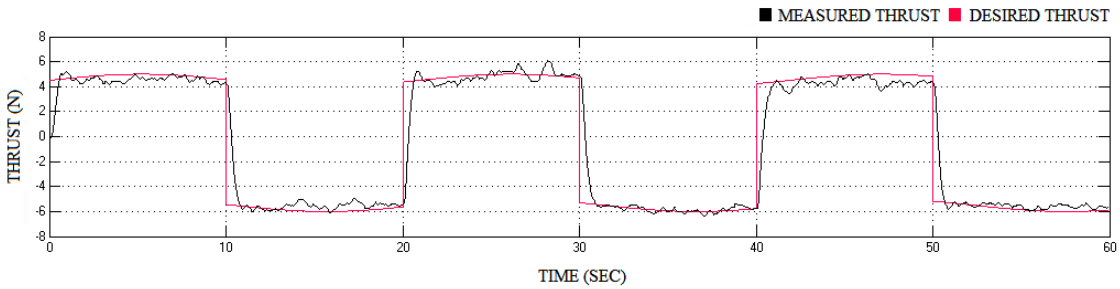

Figure 5. 2. Trust tracking result at nominal condition

As a result of these tests, fixed feed-forward controller part of proposed thruster controller's tuning process was completed. According to results which illustrated in the Figure 5.2, for both positive and negative thrust demands, open-loop controller was given acceptable results. Tuned open-loop controller was used in dynamic tests as open-loop feed-forward controller part of velocity feed-back thrust controller.

5.4. Dynamic Thrust Control Tests

Tests were conducted to validate the dynamic performance of the proposed controller when the propeller was subject to rapidly changing advance velocities in calm water with time-varying advance velocity V_a and thrust demand T_d. The controller was experimented using custom thrust demand signal which included a sinusoidal signal with amplitude of 1N and frequency of 1 rad/sec plus 4N for positive demands and -4N for negative demands. During these tests, advance velocity V_a which is the velocity of water flow at output of nozzle, was assumed to be laminar and homogeny throughout the projection area of propeller surface and equal to vehicle speed u. The ambient effect thruster was driven by a sinusoidal current commands (max: 1.52 A, min: 0.72 A) in order to make advance velocity to time varying parameter. Current values of the ambient effect thruster were directly fed to controller to obtain real-time incoming flow velocity. To realize that, the relation between ambient effect thruster current value and advance velocity, was used.

5.4.1. Positive Advance Velocity & Positive Shaft Speed Tests

Experiments were conducted under time varying positive thrust demand while propeller was subjected to variable positive incoming flow velocity. Controller and test-setup parameters were given in section 5.1 and 5.2 in this Chapter. Ventilation and cavitation were not observed during these tests. Also noise on the thrust force signal was recorded under the tolerable values of measurement. All tests were performed for at least 20 seconds. Thrust tracking and velocity error results of these tests are illustrated in Figures 5.3 and 5.4.

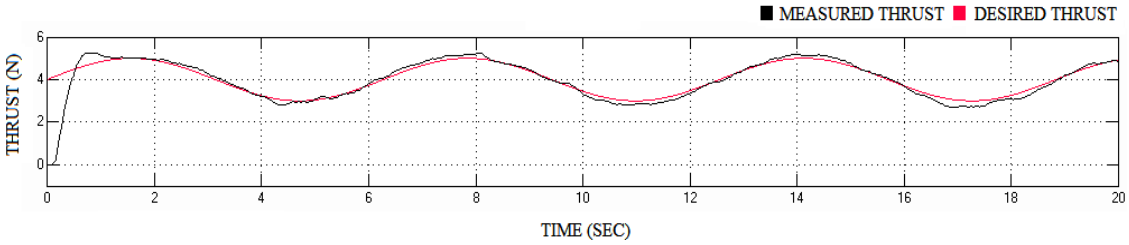

Figure 5. 3. Thrust tracking results of controller at first quadrant

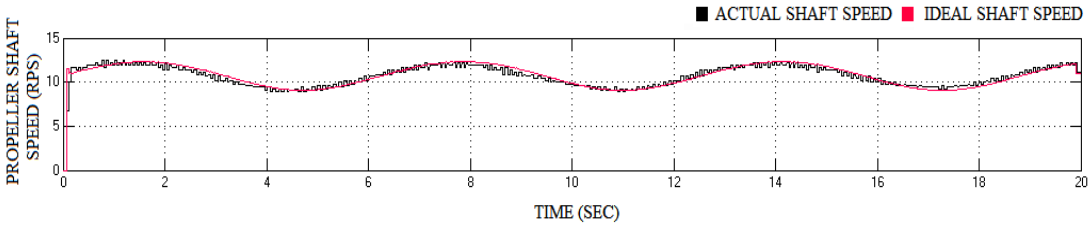

Figure 5. 4. Velocity error results of controller at first quadrant

More than 20 tests were repeated for this condition and similar results were recorded. Results from these tests show that controller provided satisfactory thrust tracking results for positive time-varying thrust demand and advance velocity navigation. First-quadrant condition's advance number J, thrust coefficient K_T /10 and advance velocity V_a with respect to time graphics are shown in Figure 5.5.

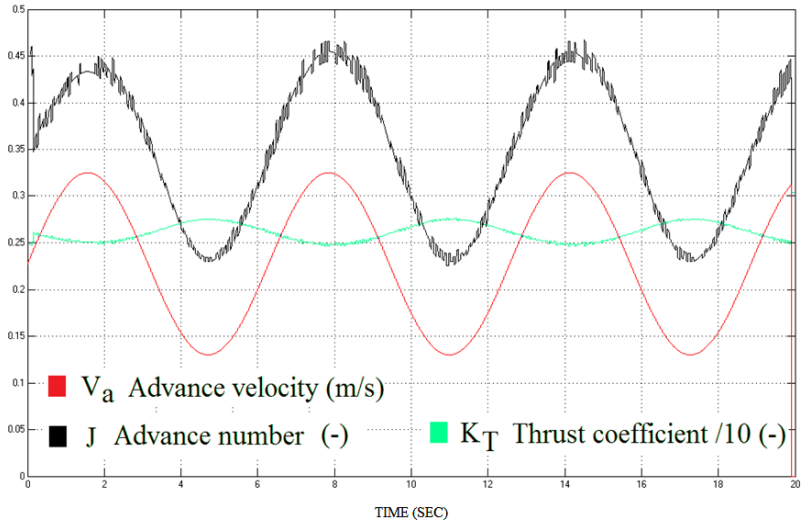

Figure 5. 5. First quadrant test: V_a, J and K_T diagram

Additionally, conventional open-loop controller with same controller parameters was tested in this quadrant to achieve a comparison between conventional thrust controller and velocity feed-back controller. Thrust and velocity tracking results of fixed feed-forward open-loop controller are shown in Figures 5.6 and 5.7 respectively.

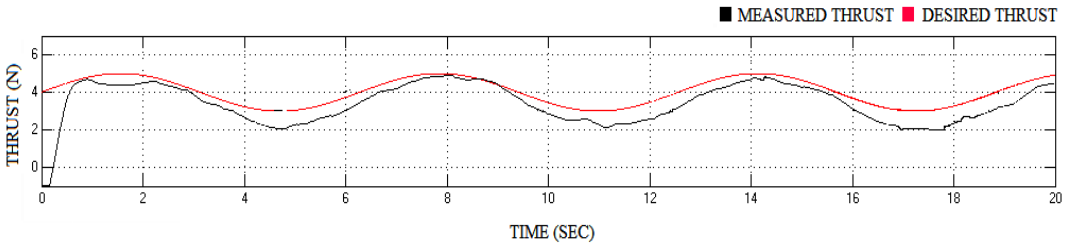

Figure 5. 6. Fixed forward controller's thrust tracking result at first quadrant

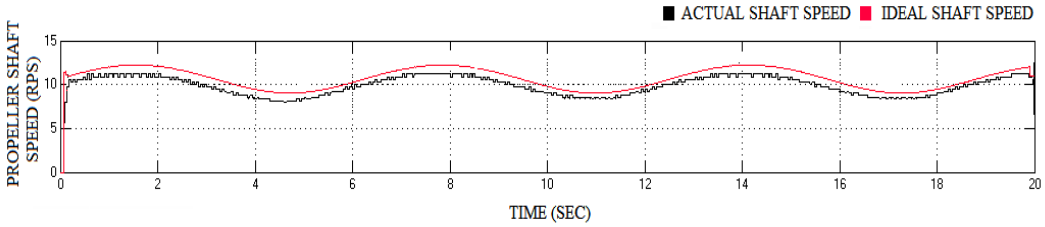

Figure 5. 7. Fixed forward controller's velocity error result at first quadrant

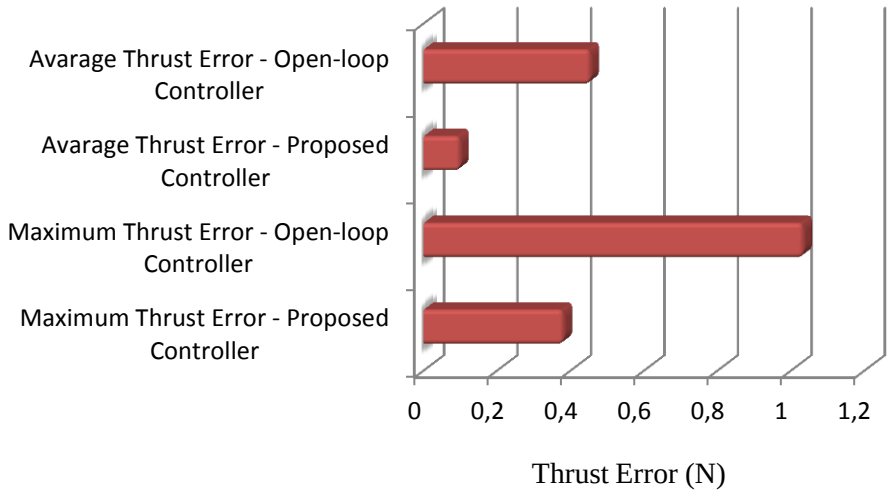

Figure 5. 8. Thrust force matching error comparison at first quadrant

The proposed controller's test results were compared with the conventional open-loop controller, which is given in Figure 5.8. The results obtained from more than 15 tests for this quadrant navigation with both open-loop and feed-back controllers showed that, the performance of the proposed controller was more reliable compared to conventional controller which did not contain model of the flow dynamics.

5.4.2. Negative Advance Velocity & Positive Shaft Speed Tests

Thruster allocation was changed into reverse direction, in order to achieve realistic negative vehicle speed effect in negative advance speed operations. Due to this modification, drag forces was increased and velocity of incoming flow from nozzle was reduced. In order to compensate these changes, controller parameters which are given in section 5.2, were re-measured. The results of thrust tracking and velocity error are displayed in Figures 5.9 and 5.10 respectively.

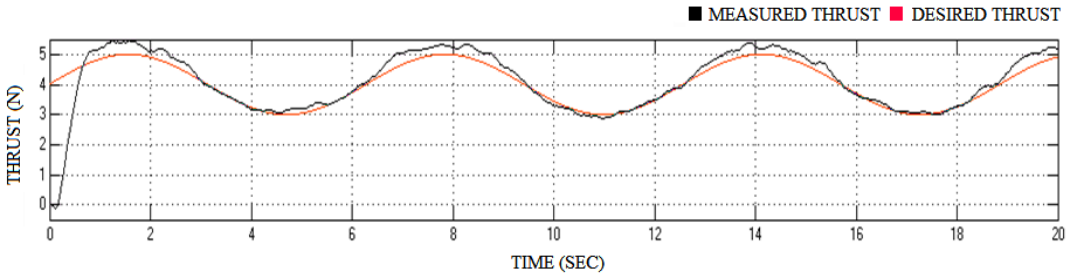

Figure 5. 9. Thrust tracking result of controller at second quadrant

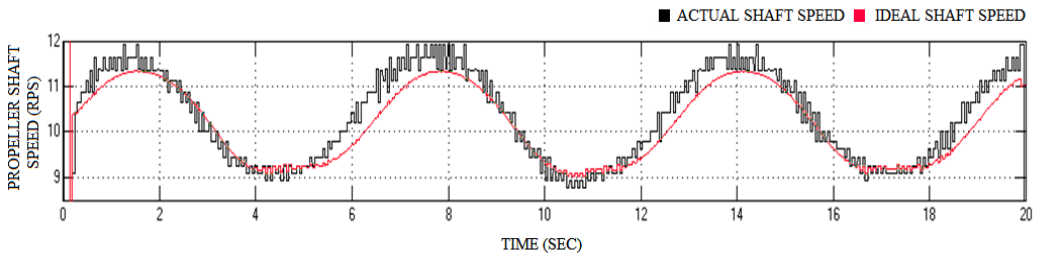

Figure 5. 10. Velocity error result of controller at second quadrant

Controller was suffered by the vibration problem that was likely to occur in positive advance velocity and negative shaft speed condition. Addition to this, back side of the control thruster blockaded the incoming axial flow current. Due to this reason advance velocity was changed dramatically. Since in the experiments, measurement of the advance velocity was only obtainable from ambient effect thruster current values, the relation between advance velocity and current of ambient effect thruster was re-configured for this quadrant navigation.

More than 50 tests were conducted to achieve optimum controller parameters which provide fastest possible velocity tracking while stabilizing the system.

Especially at the some parts of thrust demand tracking, the re-tuned proposed controller was provided unsatisfactory thrust tracking and speed tracking results compared to same controller's first-quadrant results. This was mainly caused by the existence of the vibration on the experimental test set-up structure. According to positive advance velocity & negative propeller shaft speed tests, advance number J, thrust coefficient $K_T/10$ and advance velocity V_a with respect to time diagrams are given in Figure 5.11.

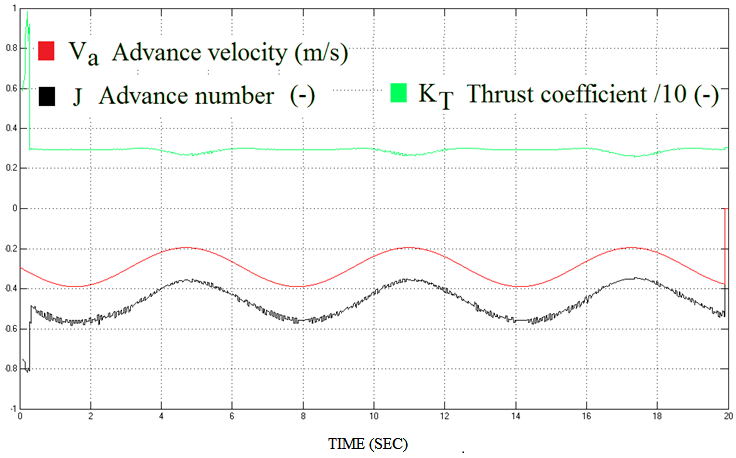

Figure 5. 11. Second quadrant test: V_a, J and K_T diagrams

Thrust control tests with fixed open-loop feed-forward controller were also conducted for this flow condition. Thrust tracking and velocity error result of thrust control test without velocity feed-back algorithm is shown in Figures 5.12 and 5.13 respectively.

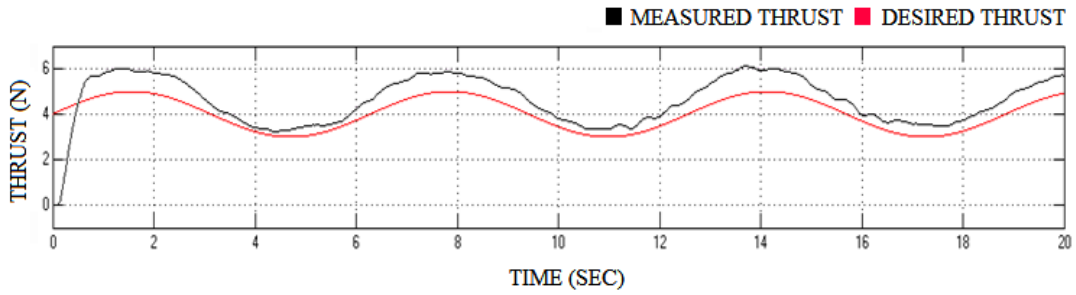

Figure 5. 12. Fixed forward controller's thrust tracking result at second quadrant

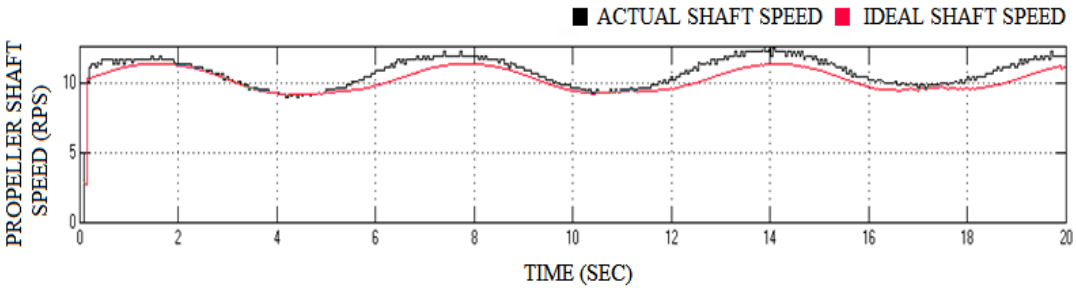

Figure 5. 13. Fixed forward controller's velocity error result at second quadrant

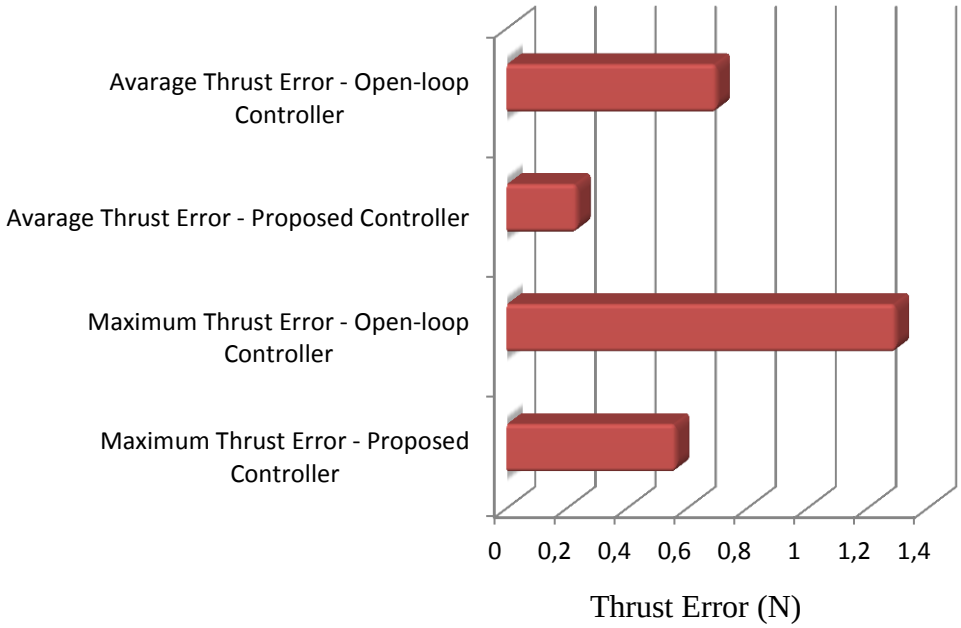

Figure 5. 14. Thrust force matching error at second quadrant

The comparison results of second-quadrant navigation for both open-loop and feed-back controllers are given in Figure 5.14. This result showed that controller's performance in second quadrant was reduced compared to results at first quadrant but still provided better thrust tracking accuracy than the conventional open-loop controller.

5.4.3. Positive Advance Velocity & Negative Shaft Speed Tests

Experiments were conducted in positive advance speed and negative propeller shaft speed condition with same controller parameters as in first quadrant feed-back controller tests. Thrust tracking results and velocity error graphics are given in Figures 5.15 and 5.16 respectively. Advance number J, thrust coefficient $K_T/10$ and advance velocity V_a with respect to time graphics for this navigation condition are given in Figure 5.17.

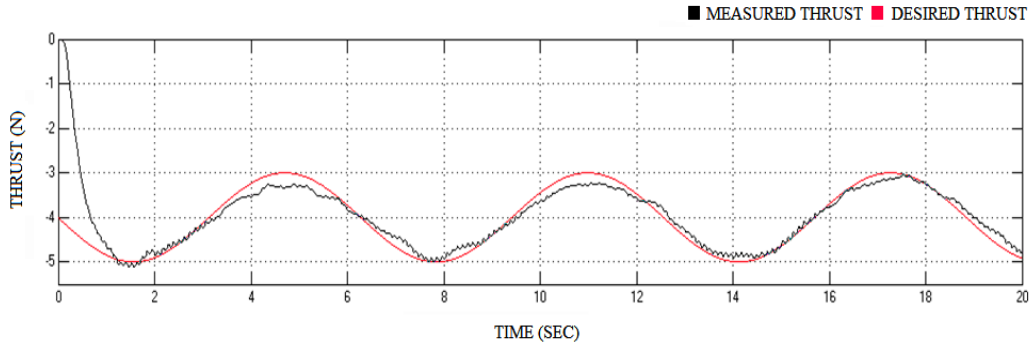

Figure 5. 15. Thrust tracking result of controller at third quadrant

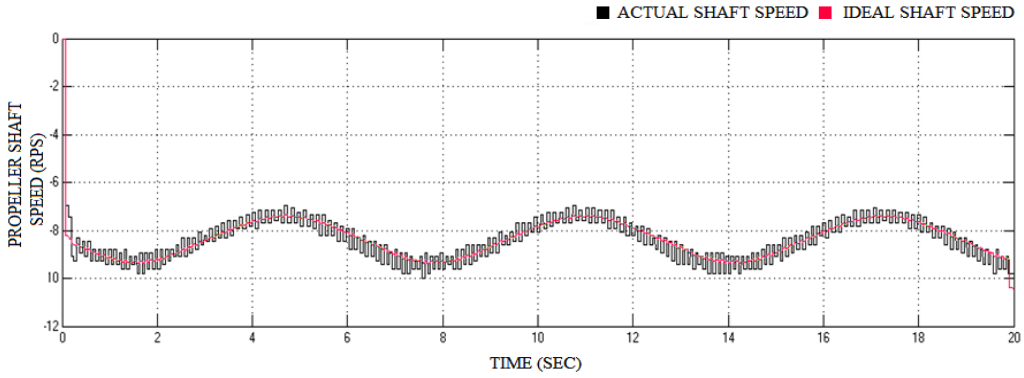

Figure 5. 16. Velocity error results of controller at third quadrant

Positive advance speed - negative shaft speed and negative advance speed - positive shaft speed conditions, the vibration problem was occurred on the metal structure of experimental test-setup. This was mainly caused by limitations of the experimental setup configuration for anti-directional flow states. Additionally, the pressure increase which lead fluctuations on the produced thrust, was observed at output of the nozzle, because of the contra-lateral flow direction. The proposed velocity feed-back controller, especially in ideal shaft speed tracking property, was given tolerable results even in the existence of the high disturbances in this quadrant. The thrust fluctuations were observed during 20 seconds test interval which is presented in Figure 5.15. These fluctuations were mainly caused by the high pressure at the nozzle output. The vibration of acceleration nozzle also generated waves on water surface which gave the disturbances on the thrust measurement signal of the force sensor.

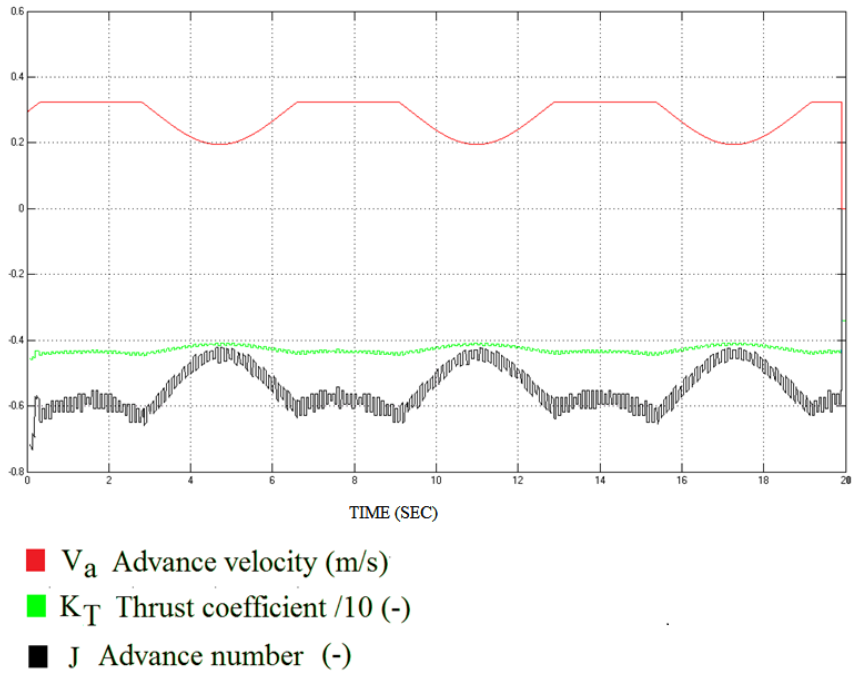

Figure 5. 17. Third quadrant tests: V_a, J and K_T diagrams

According to the results for this quadrant condition, designed experimental test setup configuration was not suitable for this flow scenario in order to achieve precise control on the thrust force. Main reason for that was the non-negligible contra-lateral flow effect on the experimental configuration. However ideal shaft speed tracking property of the proposed controller was given almost excellent performance even

against these high disturbances. Second-quadrant navigation condition with open-loop thrust controller's test results are given in Figures 5.18, 5.19 and 5.20.

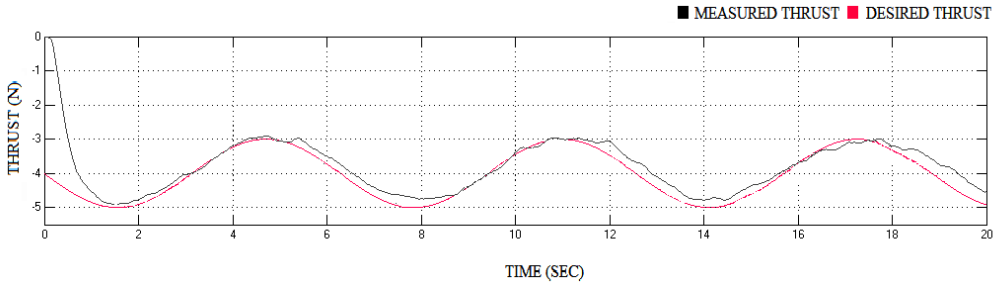

Figure 5. 18. Fixed forward controller's thrust tracking result at third quadrant

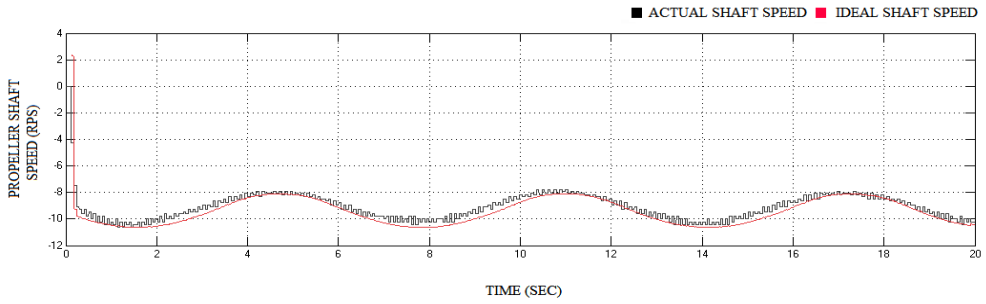

Figure 5. 19. Fixed forward controller's velocity tracking result at third quadrant

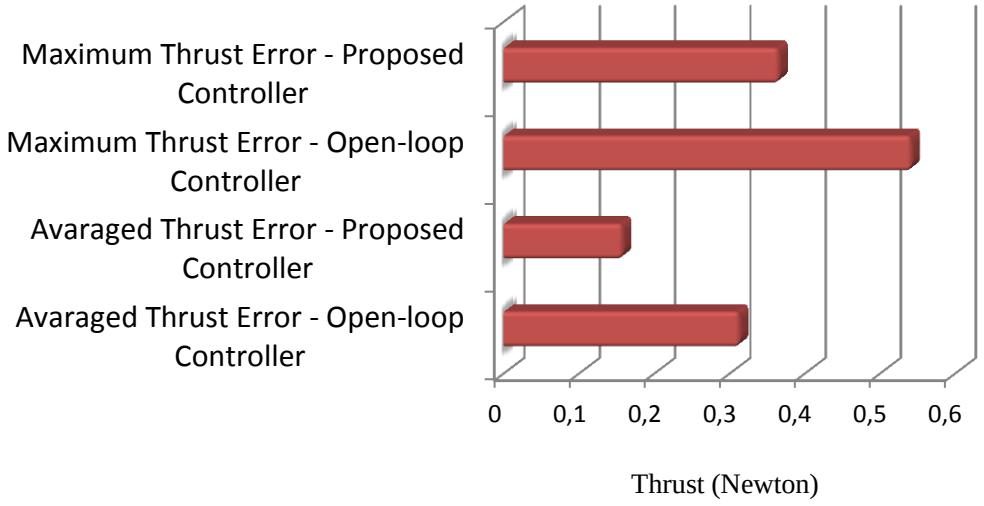

Figure 5. 20. Thrust force matching error comparison at third quadrant

As it clearly seen from Figure 5.20, close results achieved with proposed controller compared to open-loop controller for this quadrant's flow scenario. According to the results, it can be indicated that the effect of feed-back controller over produced thrust control was reduced for this condition due to incoming flow was not behaved like as it was in positive advance speed and positive thrust demand navigation scenario. Primary reason for that was the turbulences on the incoming flow path reduced the efficiency of the proposed controller.

5.4.4. Negative Advance Velocity & Negative Shaft Speed Tests

Designed thruster low-level plant controller was tested in negative advance velocity and negative shaft speed operation condition with using same experimental test setup configuration and control parameters as in section 5.4.3. Advance number *J*, thrust coefficient $K_T/10$ and advance velocity V_a with respect to time diagrams of this quadrant tests are given in Figure 5.18.

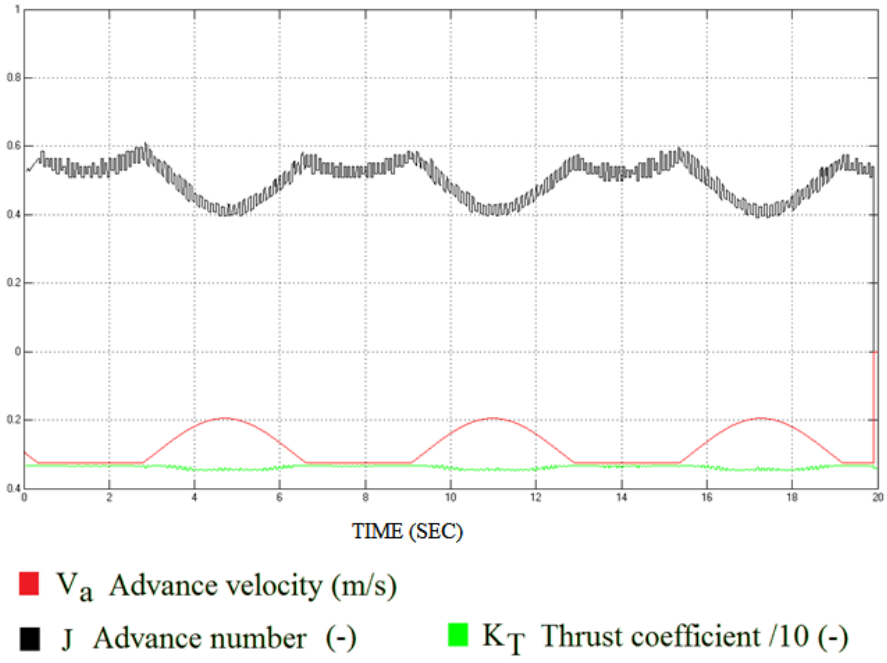

Figure 5. 21. Fourth quadrant test: V_a, J and K_T diagrams

Thrust and velocity error tracking results of this operation condition are given in Figures 5.19 and 5.20 respectively. Contrary to negative advance speed and positive shaft speed operation condition, the designed controller was given acceptable thrust and velocity tracking results.

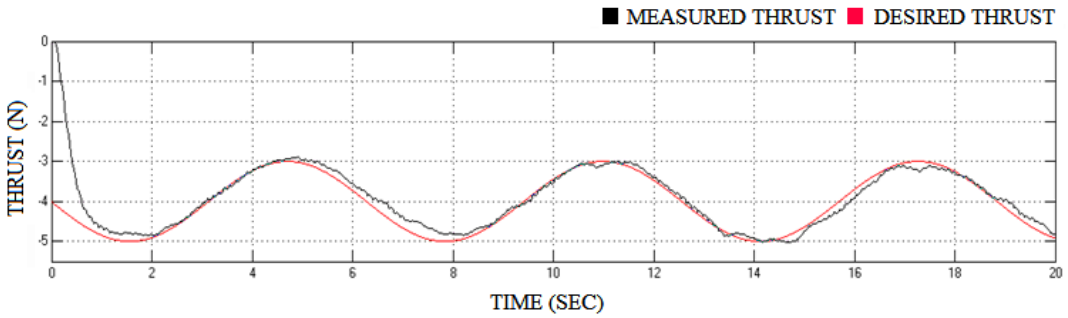

Figure 5. 22. Thrust tracking result of controller at fourth quadrant

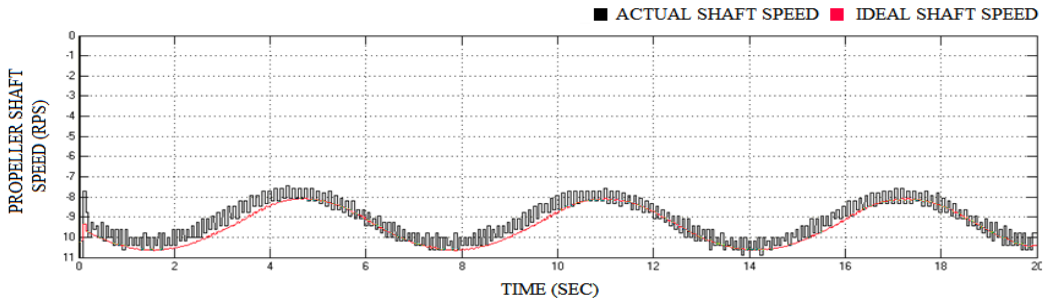

Figure 5. 23. Velocity error result of controller at fourth quadrant

For this flow condition, tests with conventional open-loop controller were also conducted to achieve a comparison between two low-level UMV controllers. Thrust and velocity error tracking results of conventional controller are given in Figures 5.24 and 5.25 respectively. Additionally, thrust matching error comparison chart is given in Figure 5.26. According to the chart, thrust tracking ability was improved by using the proposed controller compared to open-loop feed-forward thruster controller.

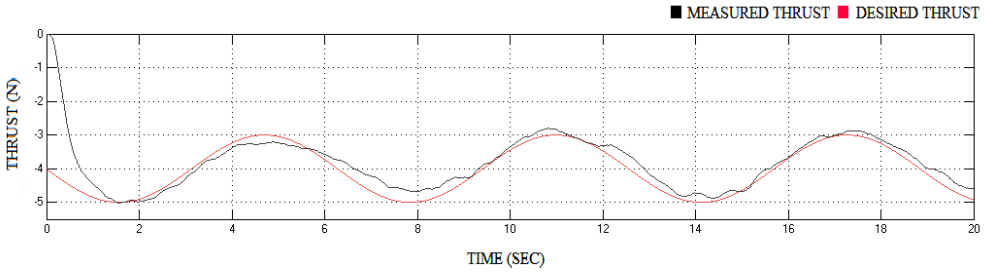

Figure 5. 24. Fixed forward controller's thrust tracking error at fourth quadrant

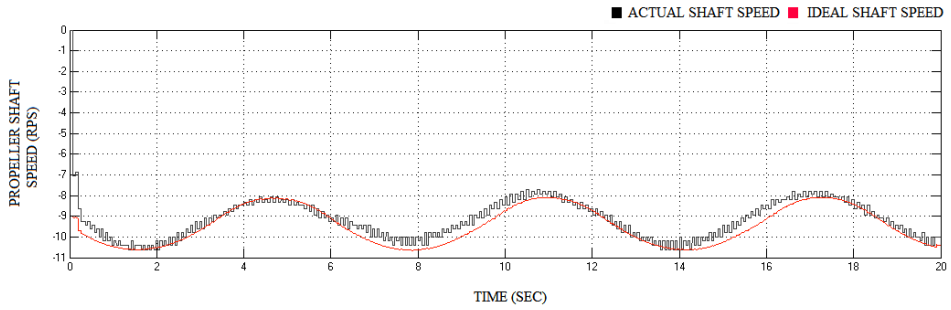

Figure 5. 25. Fixed forward controller's velocity error result at fourth quadrant

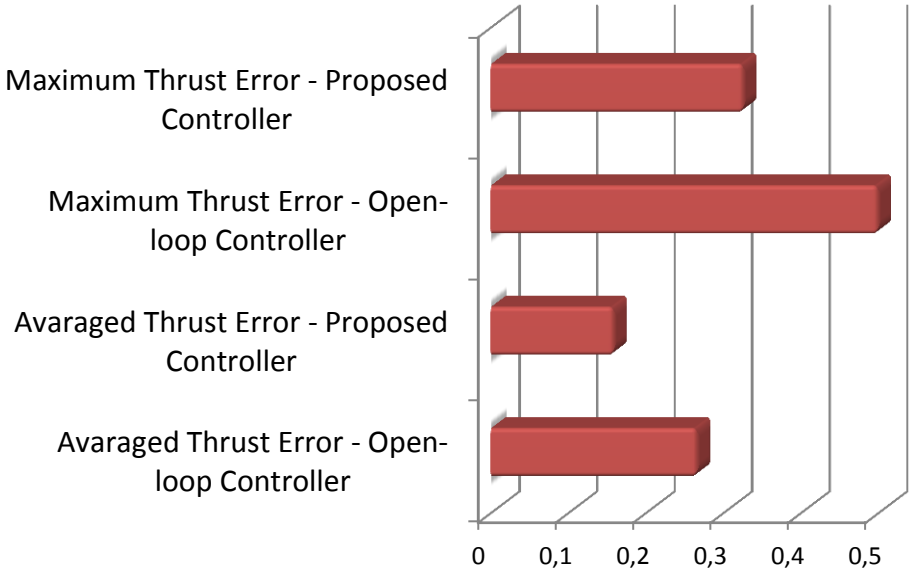

Figure 5. 26. Velocity error result of controller at fourth quadrant

5.5. Controller Performance Summary

Thrust control tests with and without velocity feed-back controller were experimented for all flow navigation conditions. For each condition, these tests were repeated for more than 20 times and the results were averaged to display thrust tracking graphics. According to these results, conventional open-loop feed-forward and the proposed feed-back controller's averaged thrust tracking errors for all operational quadrants were calculated and given in Figures 5.27 and 5.28 respectively.

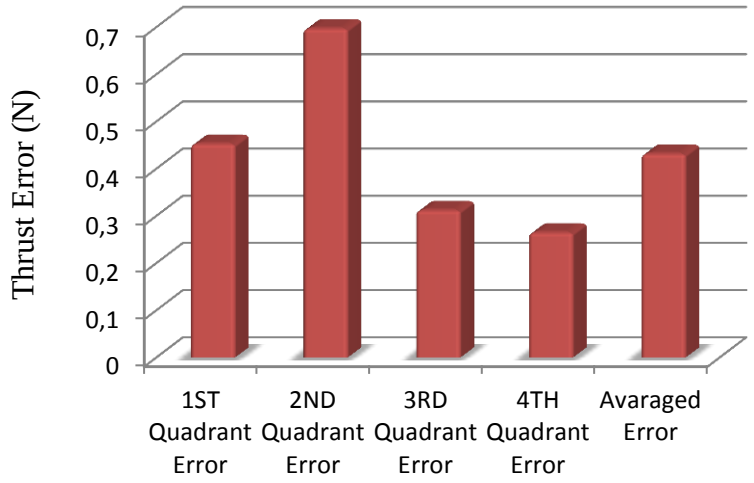

Figure 5. 27. Conventional controller's thrust tracking errors

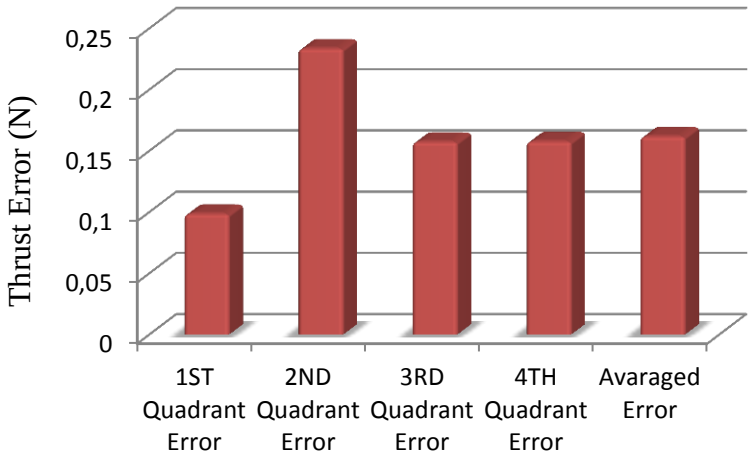

Figure 5. 28. Proposed controller's thrust tracking errors

According to these results, maximum thrust tracking error was recorded at negative advance velocity and positive shaft speed operational condition for both proposed feed-back and conventional open-loop thruster low-level controllers. In this operation quadrant, because of the contra-directional flow state, high turbulences and vibration which could count for the main reasons for thrust tracking mismatch, were noticed. Additionally, thrust tracking improvement of the proposed feed-back controller compared to the conventional open-loop controller was also measured and given for all operational quadrants in Figure 5.29.

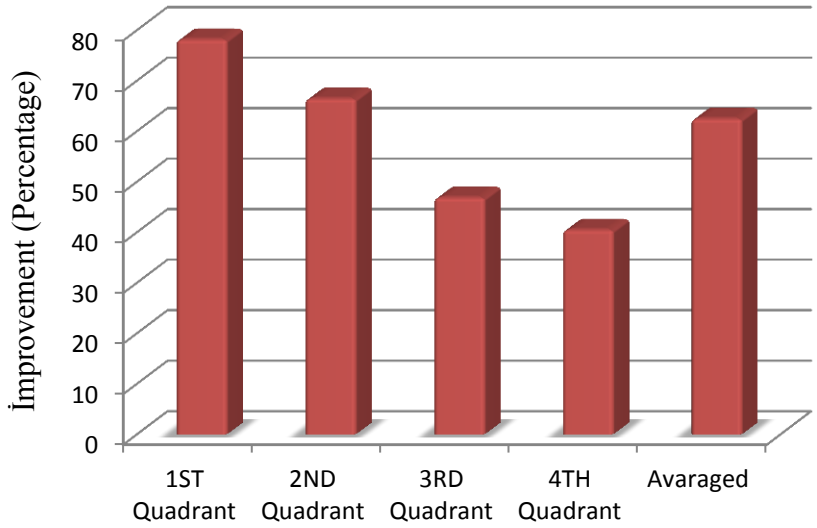

Figure 5. 29. Proposed controller's thrust tracking improvement

According to this graph, maximum thrust tracking improvement of the proposed controller was obtained in the first-quadrant operation condition while the fourth-quadrant improvement was the worst one. It was also observed that the second-quadrant's thrust tracking improvements by feed-back controller was approximately %66 where the biggest thrust tracking error was recorded. In general, the proposed feed-back thruster low-level controller gave averaged %62.5251 tracking improvement for all navigation conditions compared to the conventional open-loop thruster controller. From these results, it can be stated that the designed feed-back model-based thruster low-level controller had a significant contribution to thrust tracking ability of UMV thrusters for all kinds of operational condition.

CHAPTER 6

CONCLUSIONS

This thesis focused on the control of a propeller-based electrical-driven marine thruster with a velocity feed-back algorithm. The main purpose of this thesis is to demonstrate the importance of the low-level thruster controller over whole unmanned marine vehicle's operational performance. The four-quadrant flow characteristics of a marine propeller are analyzed on an experimental test-setup. A thrust controller includes velocity feed-back algorithm is designed based on these characteristics. The proposed velocity feed-back controller and conventional open-loop thrust controllers are tested on five different flow scenarios and the results were discussed.

According to experimental tests' results, thrust controller with velocity feed-back algorithm gives satisfactory thrust tracking results if the model parameters are chosen correctly. Therefore, to obtain correct model parameters, real vehicle with electrical-driven propeller-based marine thrusters, long towing basins, wave generators and towing methods can give better approximations.

In the tests, the proposed velocity feed-back controller gave relatively tolerable results especially in second and third-quadrants of UMV operation scenarios. Because, the model parameters mismatched and the unstable pressure rises occurred on the propeller disc area at the incoming flow side. In spite of the experimental test-setup and propeller model limitations, the proposed velocity feed-back thrust controller gave satisfactory results at equi-directional flow states like first and fourth-quadrant UMV operation conditions.

Using propeller characteristics as a control scheme, made the proposed controller practical and flexible. Due to these characteristics are easily obtainable from propeller manufacturers and vendors, they can be easily embedded into the controller core. Also by using these characteristics in the controller algorithm, submergence, pitch ratio of propeller and vehicle velocity can be used as a control parameter.

Another crucial point from this study is to demonstrate the importance of modeling of thrust and friction losses. Controller which uses only flow modeling is not reliable enough to use on precise UMV operations (Kim 2005). At the same time,

modeling of motor and shaft and analysis of inertia and friction should be investigated in order to achieve a precise UMV low-level control with high thrust tracking accuracy.

Additionally, this study does not contain the investigation of ventilation effects over whole thruster performance. Ventilation detection scheme, which will be crucial for USVs is required to be developed in order to reduce thrust loses which is likely to occur during in surface UMV operations.

Moreover, the designed velocity feed-back controller should be tested against variable incoming flow angles and oblique inflow conditions. It would be interesting to see how the proposed velocity feed-back controller handles this situation. If the performance drops down significantly during these conditions, this will also have an impact over thrust allocation system. In the experimental tests, since motor drivers did not able to provide high power to the thrusters, desired thrust was kept on low thrust demands approximately -8N to 8N thrust range. Due to this reason, the proposed velocity feed-back controller was not tested on conditions that require high thrust demands. Also provided incoming flow velocity from ambient effect thruster was relatively low, in order to realize the full effects of the incoming flow velocity over provided thrust force. To understand the full meaning of UMV thruster performance, tests at high thrust values and ambient flow speeds, are required to be analyzed.

Furthermore, without the examination of the effects like incoming flow angle, ventilation and interactions of the thrusters between hull, duct and pod, it can be said that the deigned controller is still incomplete and requires further works on analysis.

REFERENCES

Ådnanes, A. K., A. J. Sørensen and T. Hackmann (1997). Essential Characteristics of Electrical Propulsion and Thruster Drives in DP Vessels. In: Proc. DP Conference. Houston, Texas.

Akçakaya, H., Yıldız, H. A., Sağlam, G. and F. Gürleyen (2009). Sliding Mode Control of an Autonomous Underwater Vehicle, International Conference on Electrical Engineering Eleco 2009, Bursa Turkey.

Antonelli, G., S. Chiaverini, N. Sarkar and M. West (2001). Adaptive Control of an Autonomous Underwater Vehicle: Experimental Results on ODIN. IEEE Transactions on Control Systems Technology 9(5), 756—765.

Antonelli, G., (2006). Underwater Robots: Motion and Force Control of Vehicle-Manipulator Systems. ISBN: 13-978-3-540-31752-4.

Asgeir J. Sørensen, Øyvind Smogeli ve Eivind Ruth, "Propulsion Control Strategies for Fixed Pitch Propellers at Low Advance Speed," First International Symposium on Marine Propulsors Smp'09, Trondheim, Norway, 2009.

Bachmayer, R., L. L. Whitcomb and M. A. Grosenbaugh (2000). An Accurate Four-Quadrant Nonlinear Dynamical Model for Marine Thrusters: Theory and Experimental Validation. IEEE Journal of Oceanic Engineering 25(1).

Bakkeheim, J., Ø. N. Smogeli, T. A. Johansen and A. J. Sørensen (2006). Improved Transient Performance by Lyapunov-based Integrator Reset of PI Thruster Control in Extreme Seas. In: Proc. 45th IEEE Conference on Decision and Control (CDC'2006). San Diego, California.

Blanke, M. (1981). Ship Propulsion Losses Related to Automated Steering and Prime Mover Control. PhD thesis. The Technical University of Denmark. Lyngby, Denmark.

Blanke, M. and P. Busk Nielsen (1987). Electronic Governor Control for two stroke Engines. In: Nordisk Sjöfartsteknisk Årsbok Svensk Sjöfarts Tidning. Vol. 40.

Blanke, M., K. P. Lindegaard and T. I. Fossen (2000). Dynamic Model for Thrust Generation of Marine Propellers. In: Proc. 5th IFAC Conference of Maneuvering and Control of Marine Craft (MCMC'00). Aalborg, Denmark.

Caccia, M. and G. Veruggio (2000). Guidance and Control of a Reconfigurable Unmanned Underwater Vehicle. Control Engineering Practice 8, 21—37.

Defense and Industry News (2012), Defense and Industry News website, Accession Date: 05.01.2012 http://www.defenseindustrydaily.com/us-navy-spends-another-127m-for-asw-module-usvs-02735/.

Domachowski, Z., W. Próchnicki and Z. Puhaczewski (1997). The investigation of the influence of the disturbances caused by the ship propeller on the dynamic processes of the ship propulsion system. In: Marine Technology II (T. Graczyk, T. Jastrzebski and C. A. Brebbia, Eds.). pp. 237—246. WIT Press, Southampton, UK.

Durand, W. F. (Ed.) (1963). Aerodynamics Theory. Vol. IV. Dover Publications, Inc., New York.

Ekstrom, L. and D. T. Brown (2002). Interactions Between Thrusters Attached to a Vessel Hull. In: Proc. 21st Int. Conf. on Offshore Mechanics and Arctic Engineering (OMAE'02). Oslo, Norway.

Fossen, T. I. (2002). Marine Control Systems: Guidance, Navigation and Control of Ships, Rigs and Underwater Vehicles. Marine Cybernetics. Trondheim, Norway.

Fossen, T. I. and J. P. Strand (2001). Nonlinear Passive Weather Optimal Positioning Control (WOPC) System for Ships and Rigs: Experimental Results. Automatica 37(5), 701—715.

Fukuba, H., S. Morita and T. Maeda (1996). Simulation of NOx Reduction by Consolidated Control of Main Engine and CPP. Bulletin of Marine Engineering Society in Japan 24(1), 21—27.

Guibert, C., E. Foulon, N. Aït-Ahmed and L. Loron (2005). Thrust control of electric marine thrusters. In: Proc. 32nd Annual Conf. IEEE Industrial Electronics Society (IECON2005). Raleigh, North Carolina, USA.

Gutsche, F. A. (1967). Einfluss der Tauchung auf Schub undWirknungsgrad von Schiffpropellern. Schiffbauforchung 6(5/6), 256—277. In German. "Influence of Submergence on Thrust and Efficiency of Ship Propellers".

Hashimoto, J., E. Nishikawa and Z. Li (1984). An Experimental Study on Propeller Air Ventilation and Its Induced Vibratory Forces. Bulletin of Marine Engineering Society of Japan 11(1), 11—21.

Haskara, I., Ü. Özgüner and J. Winkelman (2000). Wheel Slip Control for Antispin Acceleration via Dynamic Spark Advance. Control Engineering Practice 8, 1135—1148.

Healey, A. J. and D. Lienard (1993). Multivariable Sliding-Mode Control for Autonomous Diving and Steering of Unmanned Underwater Vehicles. IEEE Journal of Oceanic Engineering 18(3), 327—339.

Healey, A. J., S. M. Rock, S. Cody., D. Miles and J. P. Brown (1995). Toward an improved understanding of thruster dynamics for underwater vehicles. IEEE Journal of Oceanic Engineering 29(4), 354—361.

Indian Defense Review (2012), Indian Defense Review website, 01.01.2012 http://www.indiandefencereview.com/defence%20industry/Unmanned-Vehicles-and- Modern-Day-Combat.html.

Johansen, T. A., T. P. Fugleseth, P. Tøndel and T. I. Fossen (2003). Optimal Constrained Control Allocation in Marine Surface Vessels with Rudders. In: Proc. 6th IFAC Conference on Maneuvering and Control of Marine Craft (MCMC'03). Girona, Spain. pp. 215—220.

Kim, J. and W. K. Chung (2006). Accurate and Practical Thruster Modeling for Underwater Vehicles. Ocean Engineering 33, 566—586.

Kort, L. (1934). Der neue Düsenschrauben-Antrieb. Werft, Reederei und Hafen 15(4), 41—43. In German. "The New Ducted Thruster".

Kruppa, C. (1972). Testing of Partially Submerged Propellers. In: 13th International Towing Tank Conference (ITTC). pp. 761—775. Report of Cavitation Committee, Appendix V.

Lehn, E. (1992). FPS-2000 Mooring and Positioning, Part 1.6 Dynamic Positioning - Thruster Efficiency: Practical Methods for Estimation of Thrust Losses. Technical Report 513003.00.06. Marintek, SINTEF, Trondheim, Norway.

Lindegaard, K.-P. (2003). Acceleration Feedback in Dynamic Positioning Systems. PhD thesis. Dept. of Engineering Cybernetics, Norwegian University of Science and Technology. Trondheim.

Lindegaard, K.-P. and T. I. Fossen (2001). A Model Based Wave Filter for Surface Vessels using Position, Velocity and Partial Acceleration Feedback. In: Proc. of the IEEE Conf. on Decision and Control (CDC'2001). IEEE. Orlando, FL. pp. 946—951.

Lindegaard, K.-P. and T. I. Fossen (2003). Fuel Efficient Rudder and Propeller Control Allocation for Marine Craft: Experiments with a Model Ship. IEEE Transactions on Control Systems Technology 11(6), 850—862.

Lloyd, A. R. J. M. (1998). Sea keeping; Ship Behavior in Rough Weather. RPM Reprographics, Sussex, UK.

Matthieu V., Nadia A. and Luc L. (2008). Marine Propeller Dynamics Modelling Using a Frequency Domain Approach," 5th International Multi-Conference on Systems, Signals and Devices.

Minsaas, K. J., H. J. Thon and W. Kauczynski (1987). Estimation of Required Thruster Capacity for Operation of Offshore Vessels under Severe Weather Conditions. In: Proc. 3rd Int. Symp. Practical Design of Ship and Mobile Units (PRADS'87). Trondheim, Norway. pp. 411—427.

Monster and Critics News (2012), Monster and Critics News website, 01.01.2012 http://www.monstersandcritics.com/news/usa/features/article_1570512.php/In-Pictures-Gulf-Oil-Spill-BP-s-ROV.

National Oceanic and Atmospheric Administration (2012), National Oceanic and Atmospheric Administration website, Accession date: 01.01.2012 http://www.noaanews.noaa.gov/stories2010/20100712_underwatervolcano.html.

Newman, J. N. (1977). Marine Hydrodynamics. MIT Press. Cambridge, MA.

Nilsen, R. (2006). Private conversations with Prof. Roy Nilsen, Dept. of Electric Power Engineering NTNU.

Oosterveld, M. W. C. and P. van Oossanen (1975). International Ship building Progress 22(251), 251—262.

Osaka University (2012), Osaka University website, Accession date: 05.01.2012 http://www.naoe.eng.osaka- u.ac.jp/~kato/fma_e.htm.

Petersen, J. K., (2009). Understanding Surveillance Technologies, Second Edition, ISBN: 978-0-8493-8319-9.

Pivano, L., Ø. N. Smogeli, T. A. Johansen and T. I. Fossen (2006a). Experimental Validation of a Marine Propeller Thrust Estimation Scheme for a Wide Range of Operations. In: Proc. 7th IFAC Conference on Manoeuvring and Control of Marine Craft (MCMC'06). Lisbon, Portugal.

Pivano, L., Ø. N. Smogeli, T. A. Johansen and T. I. Fossen (2006b). Marine Propeller Thrust Estimation in Four-Quadrant Operations. In: Proc. 45th IEEE Conference on Decision and Control (CDC'2006). San Diego, California.

Pivano, L., T. I. Fossen and T. A. Johansen (2006c). Nonlinear model identification of a marine propeller over four-quadrant operations. In: Proc. 14th IFAC Symposium on System Identification (SYSID'06). Newcastle, Australia.

Powersys Company (2012), Powersys Company website, Accession date: 05.01.2012 http://www.powersys.com/application-directory/marine-auxiliary.

Roberts G., Sutton R., (2006). Advances in Unmanned Marine Vehicles, ISBN-10: 0863414508, ISBN-13: 978-0863414503, Publication Date: January 31, 2006.

Ruth, E. (2005). Modeling and control of controllable pitch thrusters subject to large losses. Master's thesis. Department of Marine Technology, Norwegian University of Science and Technology — NTNU.

Ruth, E. and Ø. N. Smogeli (2006). Ventilation of Controllable Pitch Thrusters. SNAME Marine Technology 43(4), 170—179.

Ruth, E., Ø. N. Smogeli and A. J. Sørensen (2006). Overview of Propulsion Control for Surface Vessels. In: Proc. 7th IFAC Conference on Manoeuvring and Control of Marine Craft (MCMC'06). Lisbon, Portugal.

Sciavicco, L. and B. Siciliano (2000). Modeling and Control of Robot Manipulators. 2nd ed. Sprenger-Verlag. London, UK.

Smogeli, Ø. N., A. J. Sørensen and K. J. Minsaas (2006). The Concept of Anti- Spin Thruster Control. Control Engineering Practice. To appear.

Smogeli, Ø. N., A. J. Sørensen and T. I. Fossen (2004a). Design of a Hybrid Power/Torque Thruster Controller with Thrust Loss Estimation. In: Proc. IFAC Conference on Control Applications in Marine Systems (CAMS'04). Ancona, Italy.

Smogeli, Ø. N. and A. J. Sørensen (2006a). Adaptive Observer Design for a Marine Propeller. In: Proc. 14th IFAC Symposium on System Identification.

Smogeli, Ø. N., E. Ruth and A. J. Sørensen (2005a). Experimental Validation of Power and Torque Thruster Control. In: Proc. Mediterranean Conference on Control and Automation (MED'05). Limassol, Cyprus.

Smogeli, Ø. N., L. Aarseth, E. S. Overå, A. J. Sørensen and K. J. Minsaas (2003). Anti-spin Thruster Control in Extreme Seas. In: Proc. 6th IFAC Conference on Manoeuvring and Control of Marine Craft (MCMC'03). Girona, Spain. pp. 221—226.

Smogeli, Ø. N., T. Perez, T. I. Fossen and A. J. Sørensen (2005b). The Marine Systems Simulator State-Space Model Representation for Dynamically Positioned Surface Vessels. In: Proc. 11th Cong. International Maritime Association of the Mediterranean (IMAM'05). Lisbon, Portugal.

Smogeli, Ø. N., (2008). Control of Marine Propellers From Normal to Extreme Conditions. PhD thesis. Department of Engineering Cybernetics, Norwegian University of Science and Technology. Trondheim, Norway.

Society of Underwater Technologies (2012), Society of Underwater Technologies website, Accession date: 01.01.2012 http://sig.sut.org.uk/urg_uris/website/AUVpage_1.htm.

Sørensen, A. J., A. K. Ådnanes, T. I. Fossen and J. P. Strand (1997). A New Method of Thruster Control in Positioning of Ships based on Power Control. In: Proc. 4th IFAC Conference on Maneuvering and Control of Marine Craft (MCMC'97). Brijuni, Croatia.

Strand, J. P. (1999). Nonlinear Position Control Systems Design for Marine Vessels. PhD thesis. Department of Engineering Cybernetics, Norwegian University of Science and Technology. Trondheim, Norway.

Wagner, H. (1925). Über die Entstehung des dynamischen Auftriebes vom Tragflügeln. Zeitschrift für angew. Math. und Mech. 5(1), 17—35. In German. "On the Origin of dynamic Lift on a Lifting Surface".

Whitcomb, L. L. and D. R. Yoerger (1999a). Development, Comparison, and Preliminary Experimental Validation of Nonlinear Dynamic Thruster Models. IEEE Journal of Oceanic Engineering 24(4), 481—494.

Whitcomb, L. L. and D. R. Yoerger (1999b). Preliminary Experiments in Model- Based Thruster Control for Underwater Vehicle Positioning. IEEE Journal of Oceanic Engineering 24(4), 495—506.

Yang, K. C. H., J. Yuh and S. K. Choi (1999). Fault-tolerant System Design of an Autonomous Underwater Vehicle — ODIN: an Experimental Study. Int. Journ. Systems Science 30(9), 1011—1019.

APPENDIX A

THRUST CONTROL SCHEME SIMULINK BLOCKS

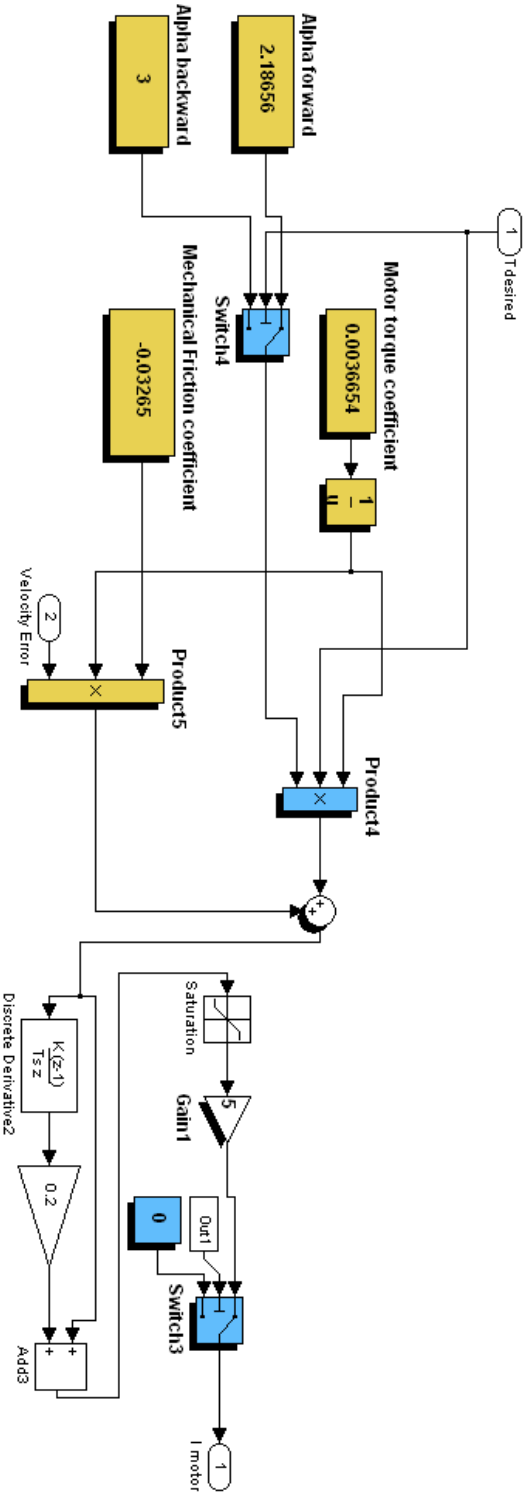

APPENDIX B

ADVANCE NUMBER AND THRUST COEFFICIENT SELECTOR SIMULINK BLOCKS

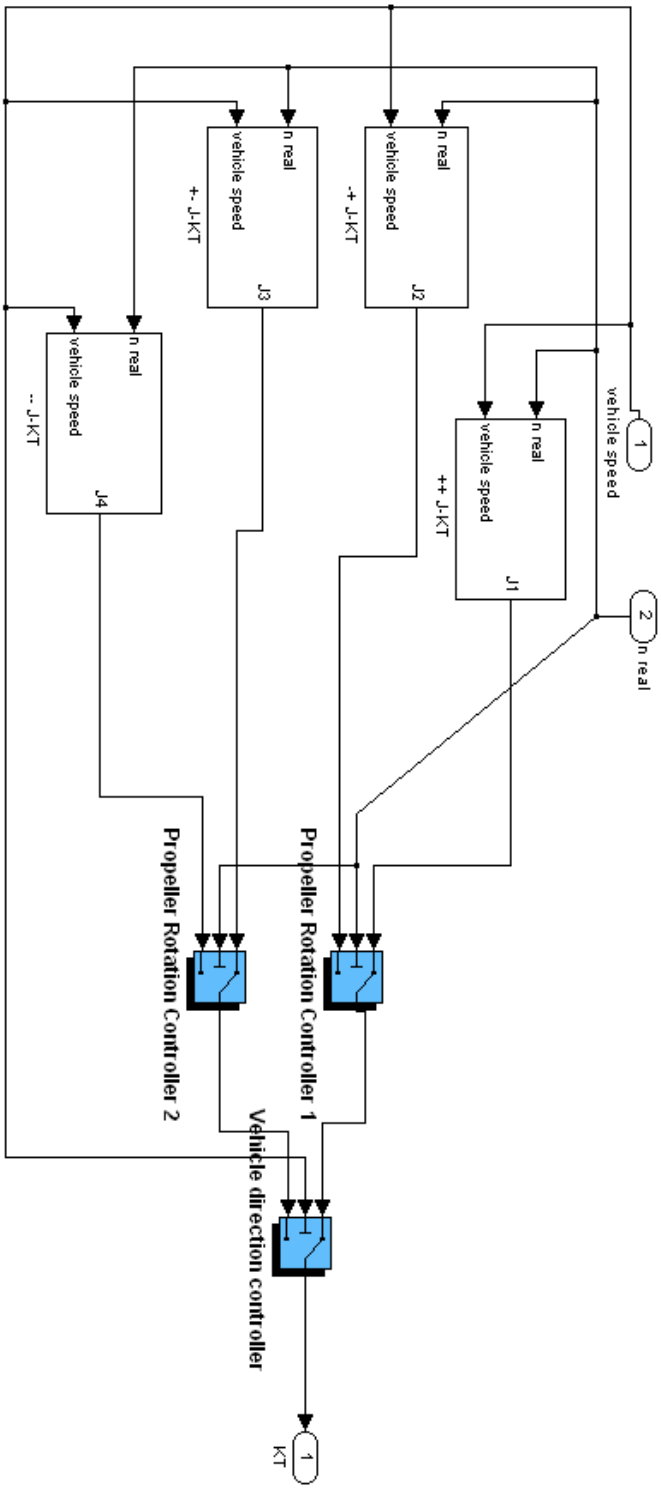

APPENDIX C

SHAFT SPEED MEASUREMENT CONSOLE SIMULINK BLOCKS

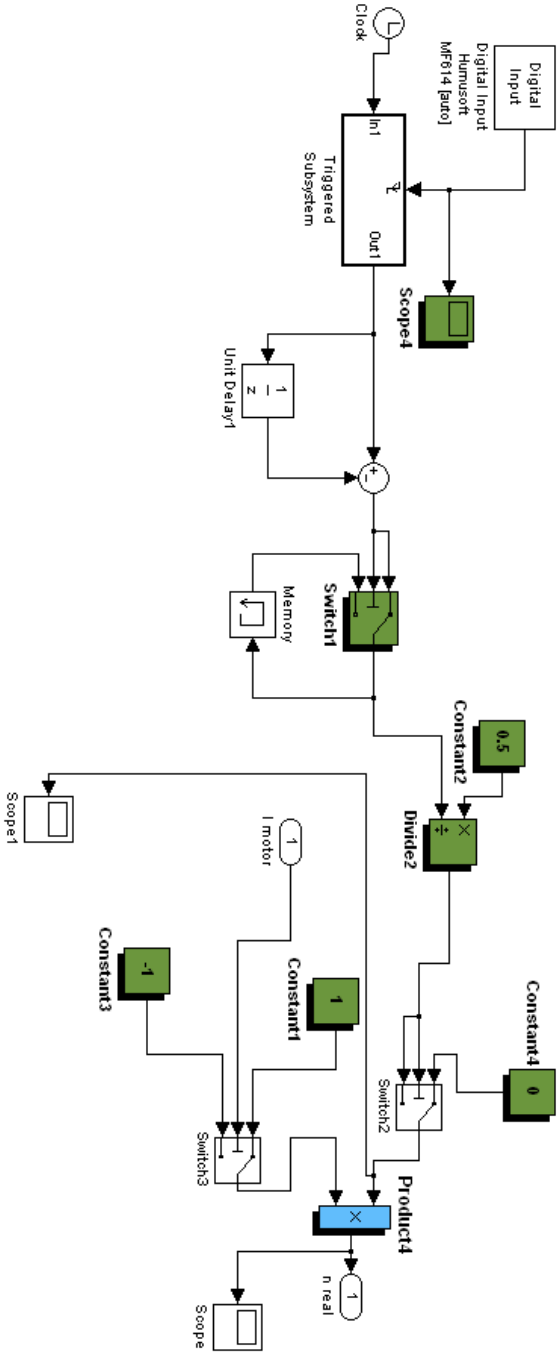

APPENDIX D

FOUR-QUADRANT THRUST CONTROLLER SIMULINK BLOCKS